

AD-A072 741

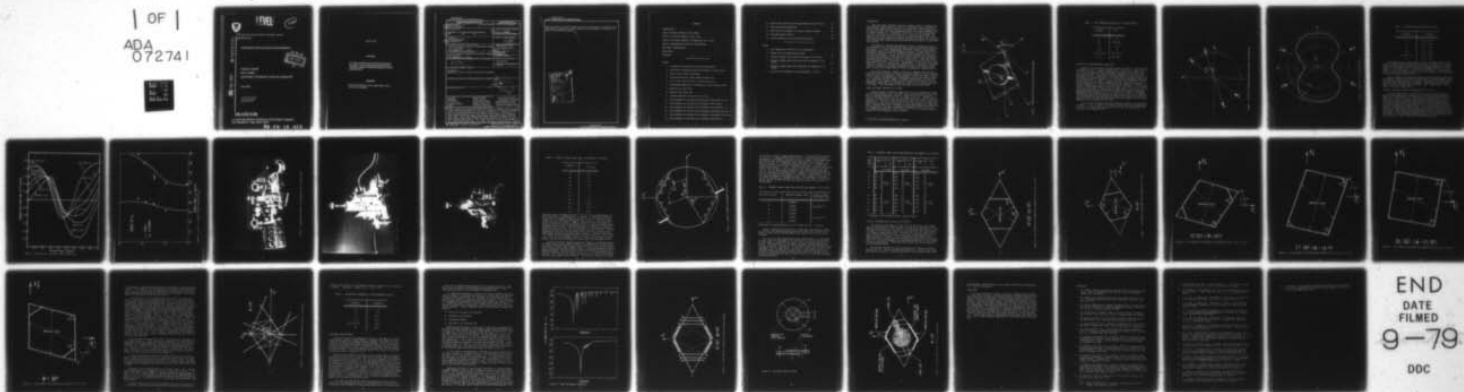
ARMY ELECTRONICS RESEARCH AND DEVELOPMENT COMMAND FO--ETC F/6 9/1
RESONATORS FOR ACCELERATION ENVIRONMENTS. (U)
JUN 79 T LUKASZEK, A BALLATO

UNCLASSIFIED

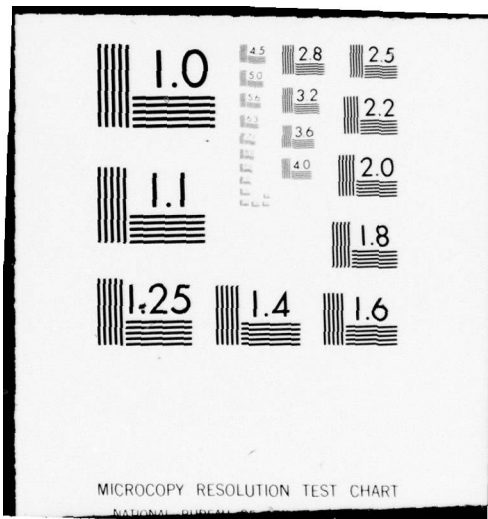
DELET-TR-79-10

NL

| OF |
ADA
072741



END
DATE
FILMED
9-79
DOC



MICROCOPY RESOLUTION TEST CHART

NATIONAL BUREAU OF STANDARDS-1963-A



LEVEL

12

RESEARCH AND DEVELOPMENT TECHNICAL REPORT

AD A 072741

DELET-TR-79-10

RESONATORS FOR ACCELERATION ENVIRONMENTS

DDC
RECEIVED
AUG 15 1979
C

Theodore Lukaszek

Arthur Ballato

ELECTRONICS TECHNOLOGY & DEVICES LABORATORY

June 1979

DISTRIBUTION STATEMENT
Approved for public release;
distribution unlimited.

DDC FILE COPY

ERADCOM

US ARMY ELECTRONICS RESEARCH & DEVELOPMENT COMMAND
FORT MONMOUTH, NEW JERSEY 07703

79 08 14 011

NOTICES

Disclaimers

The citation of trade names and names of manufacturers in this report is not to be construed as official Government indorsement or approval of commercial products or services referenced herein.

Disposition

Destroy this report when it is no longer needed. Do not return it to the originator.

UNCLASSIFIED

SECURITY CLASSIFICATION OF THIS PAGE (When Data Entered)

REPORT DOCUMENTATION PAGE		READ INSTRUCTIONS BEFORE COMPLETING FORM
1. REPORT NUMBER 14 DELET-TR-79-1b	2. GOVT ACCESSION NO.	3. RECIPIENT'S CATALOG NUMBER
4. TITLE (and Subtitle) 6 Resonators For Acceleration Environments		5. TYPE OF REPORT & PERIOD COVERED 9 Technical Report
7. AUTHOR(s) 10 Theodore/Lukaszek Arthur/Ballato		6. PERFORMING ORG. REPORT NUMBER
9. PERFORMING ORGANIZATION NAME AND ADDRESS US Army Electronics Research & Development Command ATTN: DELET-MM Fort Monmouth, N.J. 07703		8. CONTRACT OR GRANT NUMBER(s) 17 09
11. CONTROLLING OFFICE NAME AND ADDRESS US Army Electronics Research & Development Command ATTN: DELET-MM Fort Monmouth, N.J. 07703		10. PROGRAM ELEMENT, PROJECT, TASK AREA & WORK UNIT NUMBERS 11 61101 A91A 09 478
14. MONITORING AGENCY NAME & ADDRESS (if different from Controlling Office) 12 39 p		12. REPORT DATE 11 June 1979
		13. NUMBER OF PAGES 33
		15. SECURITY CLASS. (of this report) UNCLASSIFIED
		15a. DECLASSIFICATION/DOWNGRADING SCHEDULE
16. DISTRIBUTION STATEMENT (of this Report) Statement A. Approved for public release; distribution unlimited.		
17. DISTRIBUTION STATEMENT (of the abstract entered in Block 20, if different from Report)		
18. SUPPLEMENTARY NOTES		
19. KEY WORDS (Continue on reverse side if necessary and identify by block number)		
Frequency	Acoustic waves	Bulk acoustic waves
Resonators	Quartz crystals	Piezoelectric vibrators
AT cut quartz	Acceleration effects	Force-frequency efforts
Frequency Control	Doubly rotated cuts	Piezoelectric crystals
Quartz	Thickness vibrations	Pressure-frequency effects
20. ABSTRACT (Continue on reverse side if necessary and identify by block number)		
Singly rotated AT cut plates are most often used for frequency control in applications where moderate and high precision is required, but recent developments point to a greatly expanded role for doubly rotated cuts. Virtually all of these thickness mode cuts are of the form of thin circular discs mounted on their edges. Any forces communicated between the mounting supports and the quartz plate produce high stresses and stress-gradients resulting in significant frequency perturbations. This report describes crystal plate designs having a prescribed lateral contour for singly and doubly rotated plates. These		

R D C
 AUG 15 1979
 RECEIVED
 C

UNCLASSIFIED

SECURITY CLASSIFICATION OF THIS PAGE(When Data Entered)

designs provide a relatively large portion of the periphery for mounting, such that mounting stresses are greatly reduced with no detriment to the force immunity of the older-type mounts.

Accession For	
NTIS GRA&I	<input checked="" type="checkbox"/>
DDC TAB	<input type="checkbox"/>
Unannounced	<input type="checkbox"/>
Justification	
By _____	
Distribution/	
Availability	
Dist	Available on special
A	

UNCLASSIFIED

SECURITY CLASSIFICATION OF THIS PAGE(When Data Entered)

CONTENTS

INTRODUCTION	1
SINGLY AND DOUBLY ROTATED CUTS OF QUARTZ	1
EFFECTS OF IN-PLANE DIAMETRIC FORCE PAIRS	3
STUDIES TO MINIMIZE FREQUENCY PERTURBATIONS DUE TO $K_f(\psi)$	6
SPECIFIC CONFIGURATIONS FOR SELECT ORIENTATIONS	15
ADDITIONAL CONSIDERATIONS	24
CONCLUSIONS	30
REFERENCES	31

FIGURES:

1. Convention for Specifying Plate and Force Angles	2
2. Definition of Mounting Angles with Respect to Crystal Axes	4
3. Polar Plot of $K_f(\psi)$ versus Angle	5
4. Calculated $K_f(\psi)$ for Select Doubly Rotated Cuts	7
5. Loci in θ, ψ Plane of Zeros of Coefficient $K_f(\psi)$	8
6. Experimental Apparatus for Determining Force-Frequency Effect	9
7. Mounting Jig, Left View	10
8. Mounting Jig, Right View	11
9. Proposed Rhomboid Configuration for AT Cut	13
10. Plate Geometry for Minimum Force-Frequency Effect; $\theta=0^\circ$ (AT Cut)	16
11. Plate Geometry for Minimum Force-Frequency Effect; $\theta=10^\circ$	17
12. Plate Geometry for Minimum Force-Frequency Effect; $\theta=15^\circ$ (FC Cut)	18
13. Plate Geometry for Minimum Force-Frequency Effect; $\theta=19.1^\circ$ (IT Cut)	19
14. Plate Geometry for Minimum Force-Frequency Effect; $\theta=21.9^\circ$ (SC Cut)	20
15. Plate Geometry for Minimum Force-Frequency Effect; $\theta=30^\circ$	21

16. Generalized Construction Procedure Applied to $\theta=10^\circ$ Plate . . .	23
17. Mode Spectrograph Comparison	26
18. Modification of Geometry for Energy Trapping Purposes	27
19. Electrode Keyhole Pattern	28
20. Hexoid Resonator with Off-Axis Electrode Tabs	29

TABLES:

1. Zero Temperature Coefficient Cuts Investigated	3
2. Optimum Four-Point Mounting Locations	6
3. Frequency Change versus Angle Ψ for Round AT Cut Crystal . . .	12
4. Frequency Change versus Force Position for Rhomboid AT Cut Crystal	14
5. Frequency Change versus Force Magnitude for Rhomboid AT Cut Crystal	15
6. Inclination of Rhomboids to Crystallographic X_1'' Axis	24

INTRODUCTION

Almost all modern resonators used for frequency control in moderate and high precision applications are of quartz, and operate using bulk acoustic waves of the thickness shear variety. At present, the singly rotated AT cut is most often used, but recent developments point to a greatly expanded role for doubly rotated cuts. Furthermore, virtually all of the thickness mode cuts are in the form of thin circular discs. When these are mounted, the mounting clips cover relatively little of the available edge of the crystal plate and any forces communicated between the mounting supports and the quartz plate produce high stresses and stress-gradients in the vicinity of the mounting positions.

The subject of frequency perturbations in quartz vibrators produced by such external forces has received both theoretical and experimental attention previously^{1-27*}. Those investigations related the initial stress produced by mounting supports to resonance frequency changes, the contribution to long term aging, and the relation to frequency excursions produced in shock and vibration environments. Two- and four-point mount locations with respect to the plate crystallographic axes have been identified which have the potential to produce minimal frequency shifts for in-plane forces. These were identified by azimuth angles ψ in the plane of the plate for which the force-frequency coefficient $K_f(\psi)$ equals zero. Unfortunately, in practice, it has been found very difficult to position the mounting clips at the precise locations required. Mispositioning and/or increasing the area of the contact points over a larger area has been found to result in substantial frequency shifts.

This report describes in detail a design for resonator plates having a prescribed lateral contour, with mounting surfaces provided along a relatively large portion of the periphery, so that mounting stresses are greatly reduced in size, with no detriment to the force-immunity of the older type of mounting. A different lateral contour, of rhomboid configuration, for each and every member of the doubly rotated family of quartz cuts located on the zero temperature coefficient locus extending from the AT-cut to the rotated-X-cut is provided. Other advantages of this new scheme are also described.

SINGLY AND DOUBLY ROTATED CUTS OF QUARTZ

"Singly rotated" and "doubly rotated" refer to cuts oriented with respect to the crystallographic axes. The rotation(s) is/are made primarily for reasons of frequency-temperature behavior. Definitions of axes and angles involved in the specification of a cut are shown in Figure 1. Further details are given in Reference 23. When the angle θ is zero, the result is the singly rotated Y-cut. The angle θ may take on values from 0° to 30° for quartz; any other angle is equivalent to some angle in this range because of crystal symmetry. Although other doubly rotated cuts having zero temperature coefficient of frequency exist, we shall concentrate on the branch of the first order zero temperature coefficient locus where $\theta \approx +34^\circ$ to $+35^\circ$, and give specific results for the orientations listed in Table 1.

* See list of references beginning on page 31.

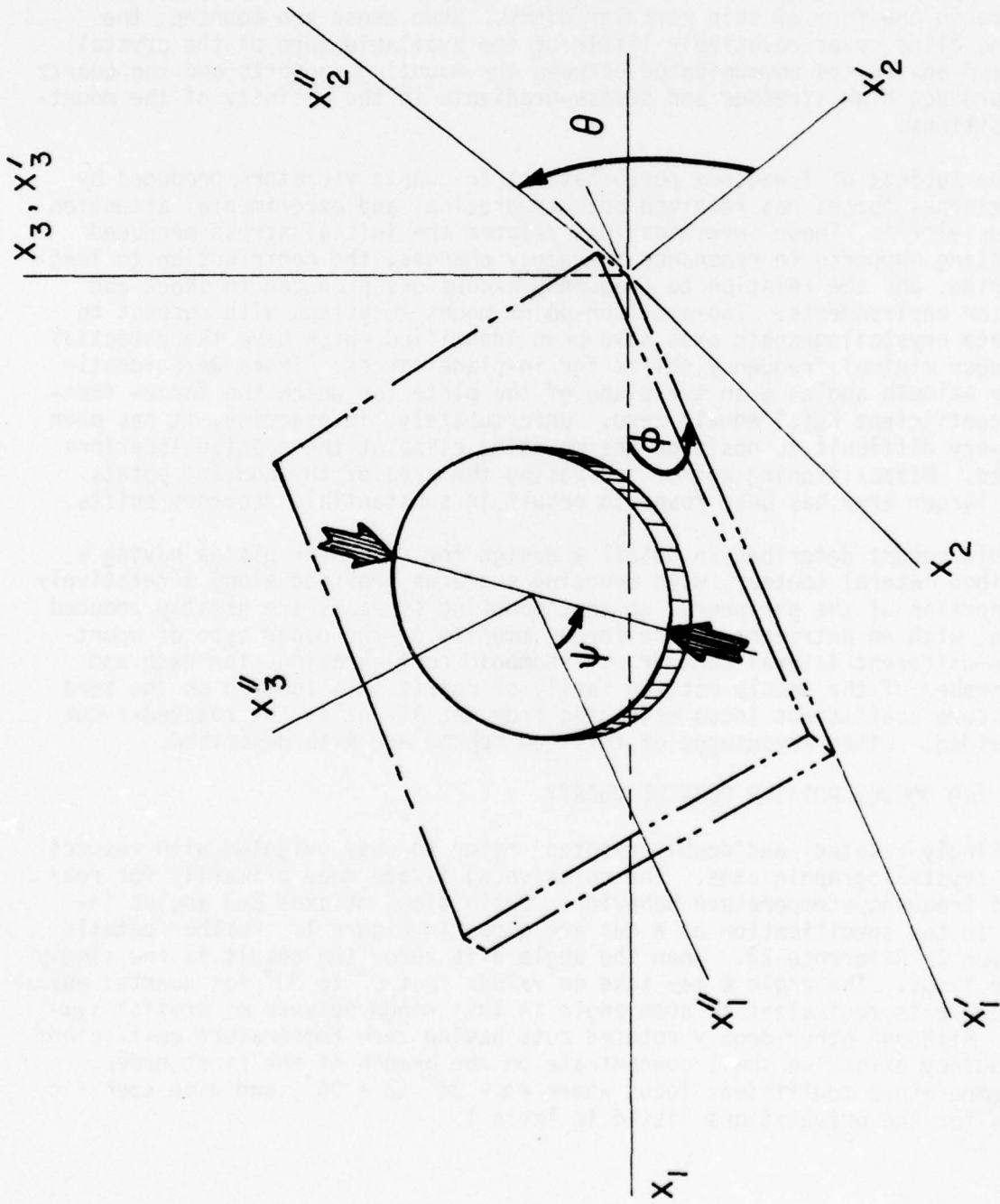


FIGURE 1. CONVENTION FOR SPECIFYING PLATE AND FORCE ANGLES.

TABLE 1. ZERO TEMPERATURE COEFFICIENT CUTS INVESTIGATED.

ϕ (degrees)	Cut
0	AT
10	10° V-Cut
15	FC
19.1	IT
21.9 to 22.4	SC; TTC; TS
30	30° V-Cut

EFFECTS OF IN-PLANE DIAMETRIC FORCE PAIRS

Consider a circular plate vibrator as shown in Figure 2. Two force-pairs are shown, F_1 and F_2 . These are point-forces. If one set of forces, say F_2 , is set to zero, and the other is applied at an azimuth ψ_1 , as shown, then the crystal frequency will change in direct proportion to the size of the force applied at F_1 . Further, the frequency change Δf is also a function of the angle ψ of the applied force. For a given plate, the quantity Δf is directly proportional to a number $K_f(\psi)$, called the force-frequency coefficient. A polar plot of $K_f(\psi)$ versus ψ is shown in Figure 3 for the AT cut. An important property of the force-frequency effect for diametric force-pairs is that of superposition. That is, the resultant Δf produced by F_1 and F_2 , from Figure 2, acting simultaneously at any two angles, as shown, is the algebraic sum of the individual Δf 's acting alone at those angles. For the AT cut, the optimum mounting location points which produced zero frequency change were determined, and are marked "A", "B", "C", and "D" in Figure 3. For doubly rotated cuts the four-point optimum mounting locations will not be symmetrically disposed about the crystal axes as shown in this figure; this only happens for the AT cut ($\theta=0^\circ$) because then the two-fold symmetry axis of quartz happens to lie in the plane of the plate.

Table 2 gives the optimum four-point mounting locations, (corresponding to points "A", "B", "C" and "D" in Figure 3), which coincide with the angles at which $K_f(\psi)$ equals zero, not only for the AT cut, but for the family of cuts that are of interest here.

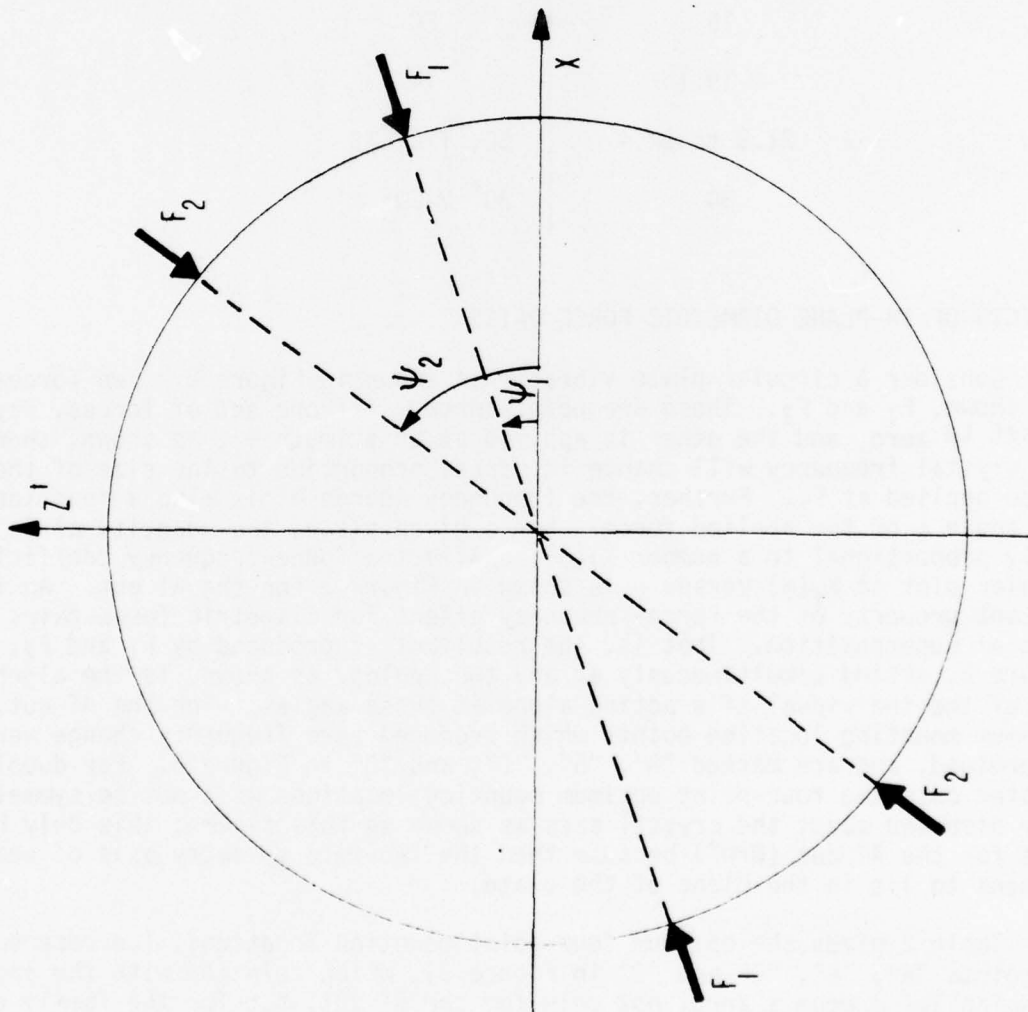


FIGURE 2. DEFINITION OF MOUNTING ANGLES WITH RESPECT TO CRYSTAL AXES.

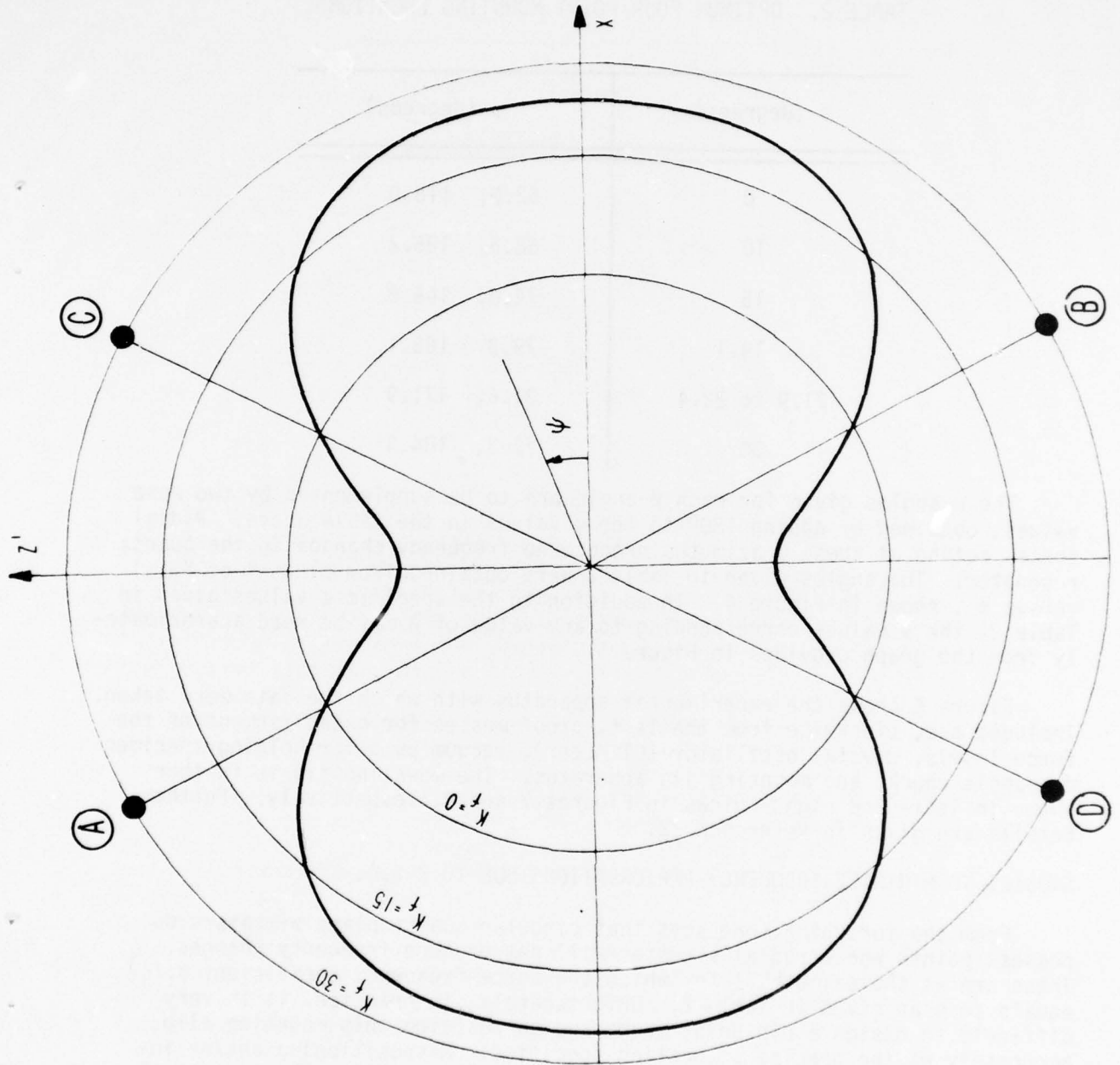


FIGURE 3. POLAR PLOT OF $Kf(\psi)$ VERSUS ANGLE ψ .

TABLE 2. OPTIMUM FOUR-POINT MOUNTING LOCATIONS.

ϕ (degrees)	ψ (degrees)
0	62.0, 118.0
10	68.5, 125.2
15	74.8, 148.8
19.1	79.3, 163.1
21.9 to 22.4	81.6, 171.9
30	79.3, 184.3

The ψ angles given for each ϕ angle are to be supplemented by two more values, obtained by adding 180° to the ψ values in the table above. Radial forces acting at these ψ azimuths produce no frequency changes in the quartz resonator. The angles given in Table 2 were obtained from plots²⁴ of $K_f(\psi)$ versus ψ , shown in Figure 4. In addition to the specific ψ values given in Table 2, the ψ values corresponding to any value of ϕ may be read approximately from the graph provided in Figure 5.

Figure 6 shows the experimental apparatus with which the data were taken. Included are, clockwise from the left, proof masses for establishment of the force levels, crystal oscillator (CI Meter), vacuum pump for holding specimen on sample chuck, and mounting jig apparatus. The mounting jig is further shown in left- and right- views in Figures 7 and 8, respectively. Further details are given in Reference 22.

STUDIES TO MINIMIZE FREQUENCY PERTURBATIONS DUE TO $K_f(\psi)$.

From the foregoing, one sees that circular quartz plate vibrators do possess points where radial stresses will not produce frequency changes. These are at the azimuths ψ for which the force-frequency coefficient $K_f(\psi)$ equals zero as given in Table 2. Unfortunately, in practice, it is very difficult to design a pin-point mount and to position this mounting clip accurately at the precise ψ location specified. Mispositioning and/or increasing the area of the contact points over a larger area will in general result in a substantial frequency shift. Even if pin-point mounts were achievable, they would give rise to extremely large stress effects at the contact points. As an example of mispositioning, consider an AT-cut plate of 14 mm diameter. Table 3 provides measured data on frequency sensitivity vs applied force for a two-point mount repositioned over a ψ angle range of 10° in the vicinity of $\psi = 62^\circ$, the zero force coefficient angle.

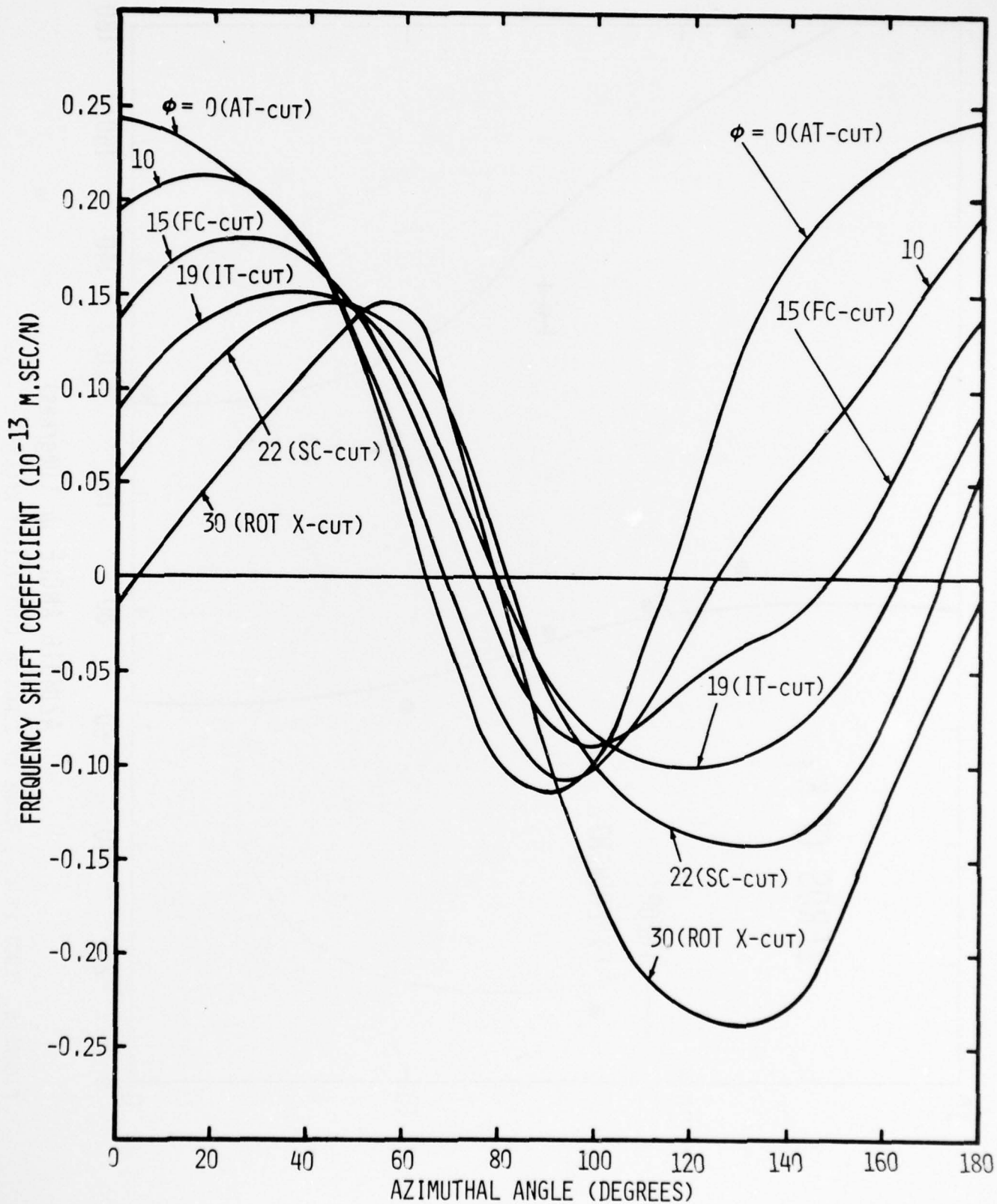


FIGURE 4. CALCULATED $K_f(\psi)$ FOR SELECT DOUBLY ROTATED CUTS.

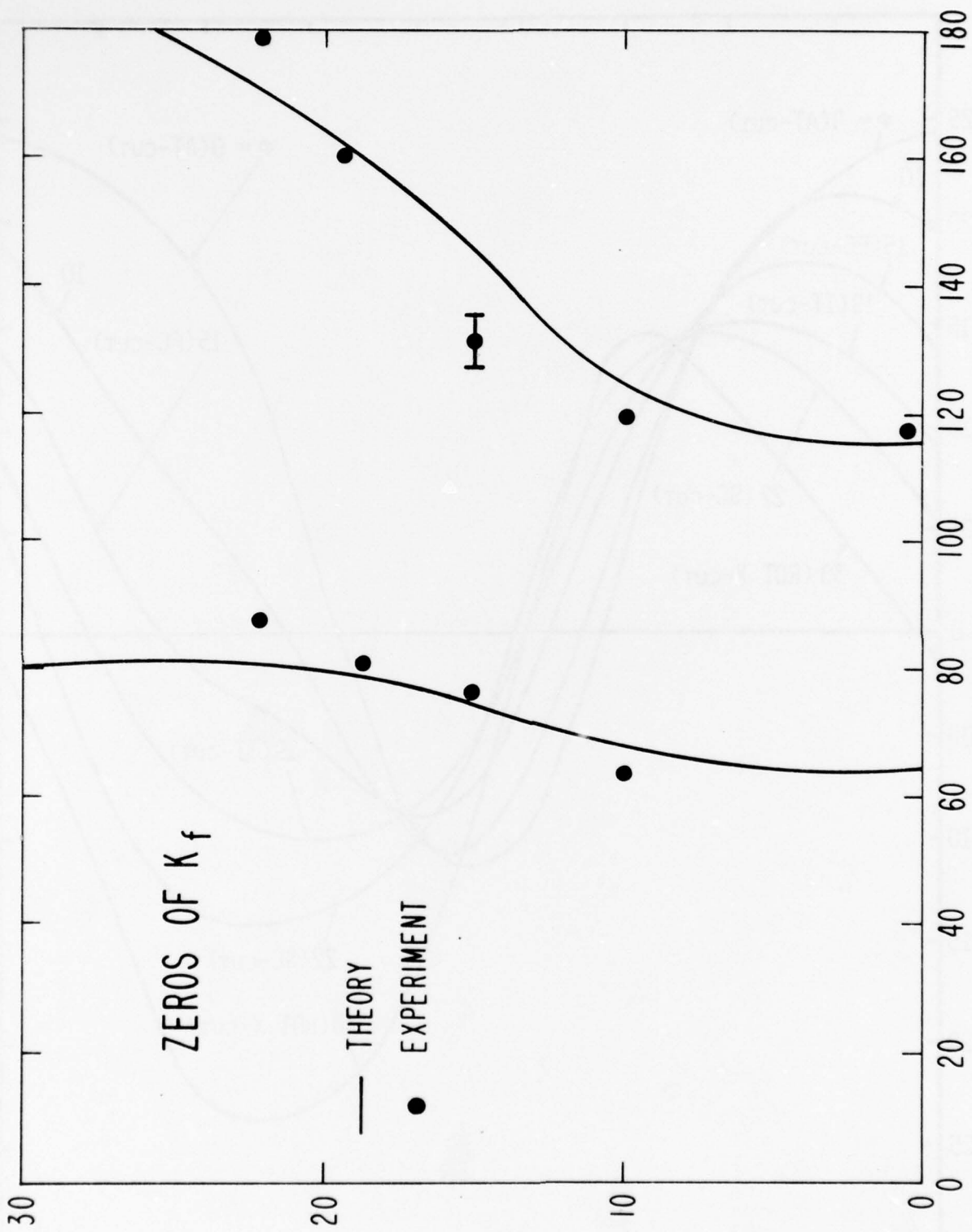


FIGURE 5. LOCI IN ϕ, ψ PLANE OF ZEROS OF COEFFICIENT $K_f(\psi)$.

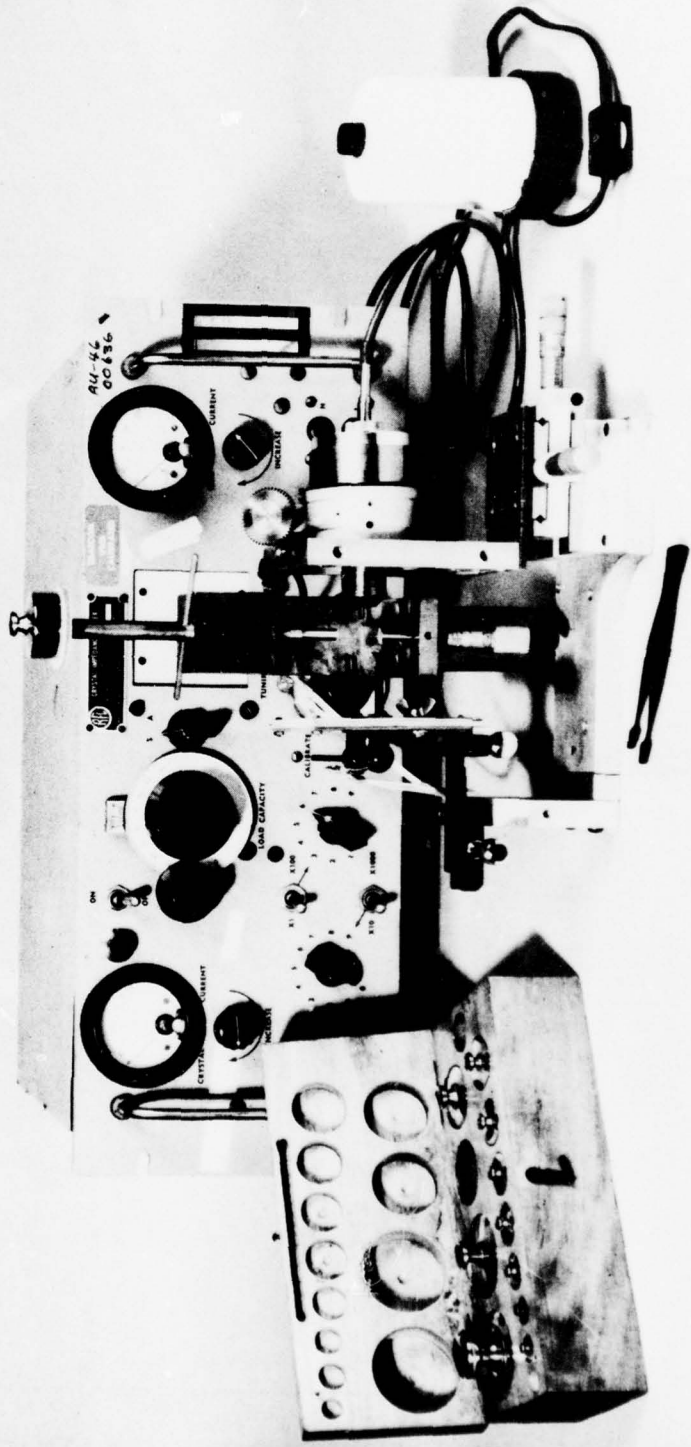


FIGURE 6. EXPERIMENTAL APPARATUS FOR DETERMINING FORCE-FREQUENCY EFFECT.

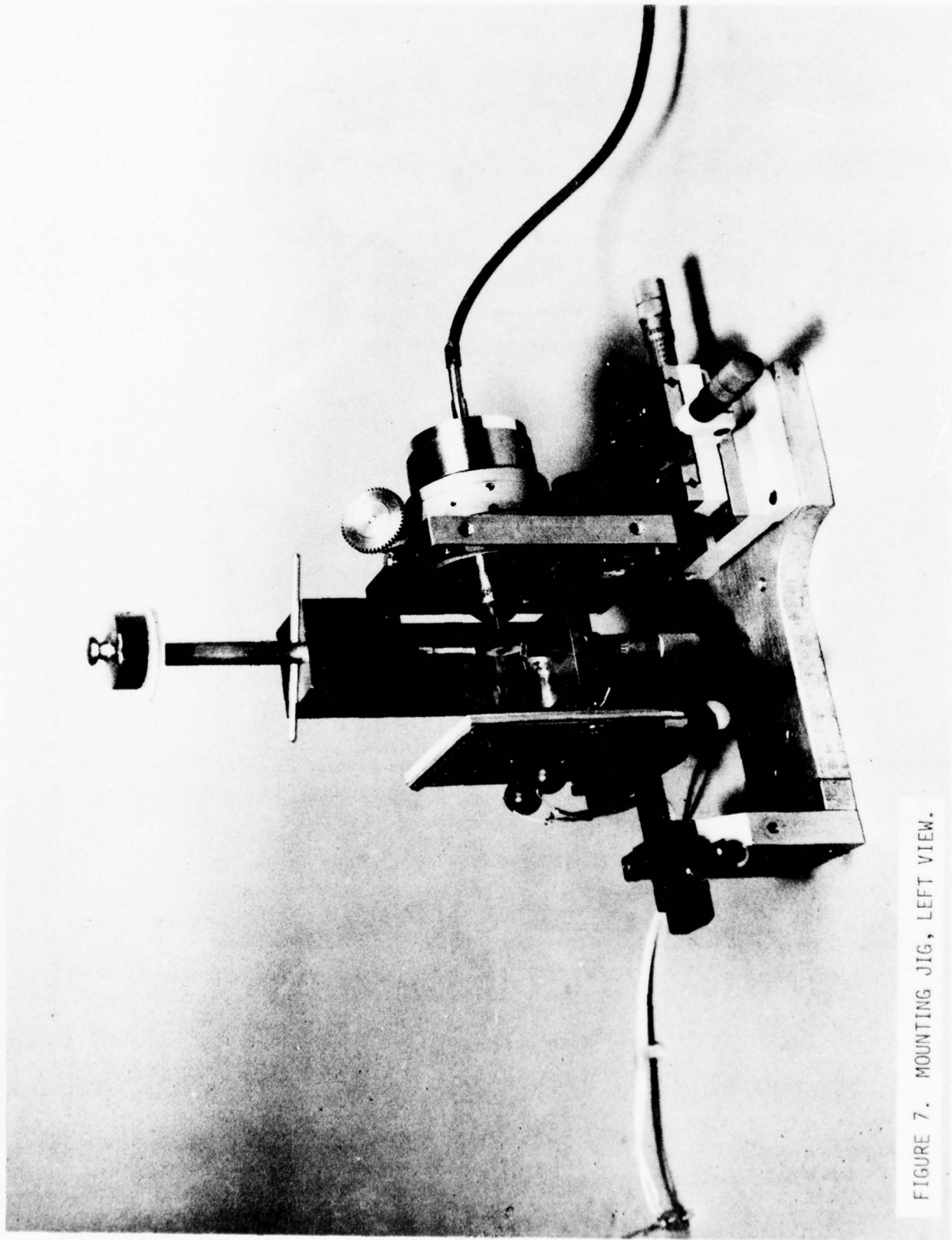


FIGURE 7. MOUNTING JIG, LEFT VIEW.

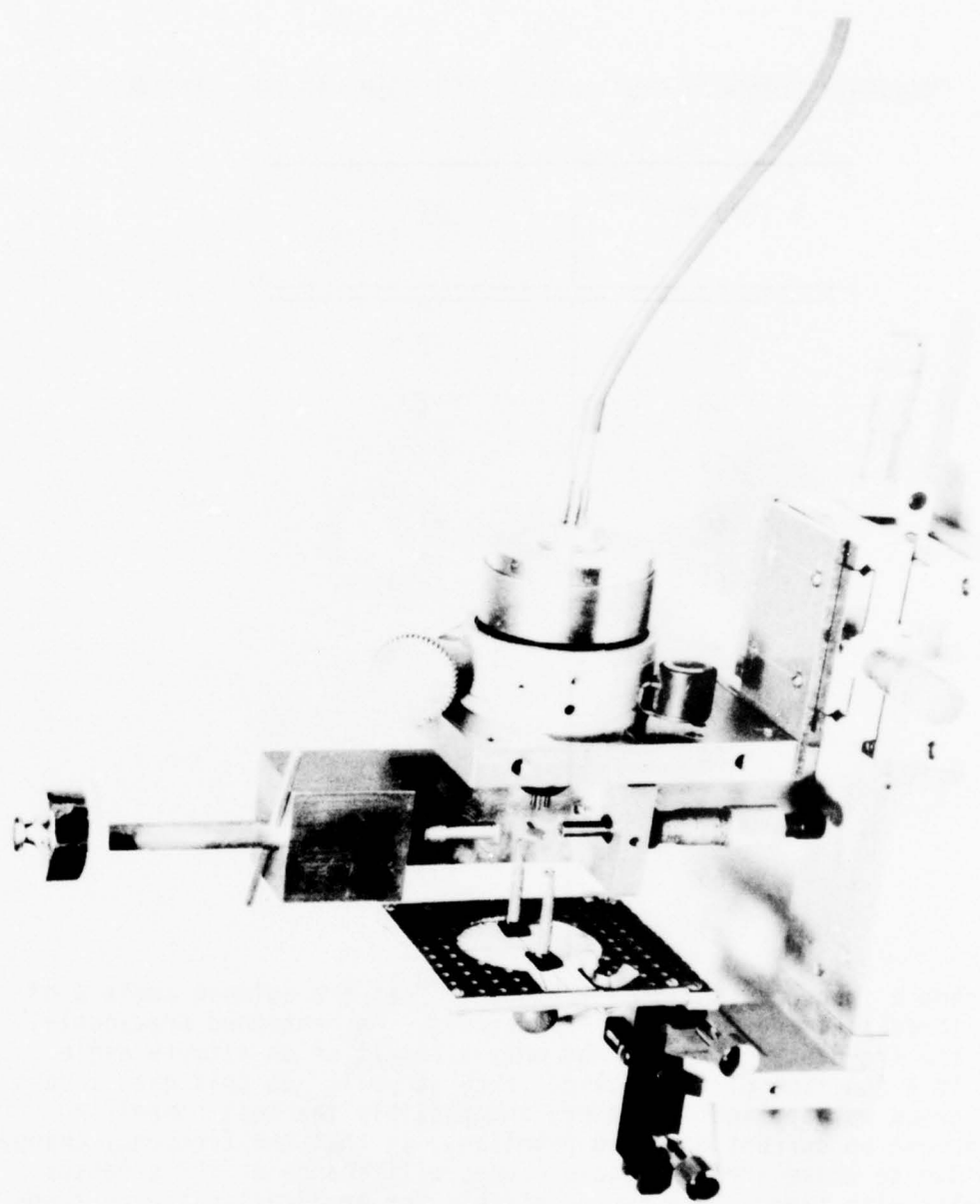


FIGURE 8. MOUNTING JIG, RIGHT VIEW.

TABLE 3. FREQUENCY CHANGE VERSUS ANGLE ψ FOR ROUND AT CUT CRYSTAL.

ψ (degrees)	$\frac{\Delta f}{f}$ (10^{-6})
57	+2.5
58	+2.0
59	+1.5
60	+1.0
61	+ .5
62	0
63	- .5
64	-1.0
65	-1.5
66	-2.0
67	-2.5

These data show a frequency shift of $\pm 2.5 \times 10^{-6}$ as the azimuth angle ψ of the applied force is changed by only ± 5 degrees. As mentioned previously, the size of the frequency change is not only a result of an azimuth angle change, but is a function of the applied force as well. In this case a mass of only 130 grams was applied. Another, and possibly the most compelling reason to improve on current mounting practices, is that the frequency change experienced due to these stress-induced causes will change as the stresses gradually relax with time. This is undesirable for applications where frequency stability due to long term aging effects are to be minimized. From the foregoing one sees that circular quartz plate vibrators do possess points where radial stresses do not affect their frequency. These are the azimuths ψ for which the force-frequency coefficient $K_f(\psi)$ equals zero. But in practice, it is, in fact, extremely difficult to mount a crystal plate at these precise locations and misalignment can cause significant frequency shifts.

Studies to minimize frequency change with respect to increasing the area of contact and/or mispositioning resulted in a geometry which allows the application of colinear forces through the crystal plate in the vicinity where $K_f(\psi)$ is zero, with minimal frequency change. Plate configurations to achieve the desired results are obtained by cutting flats tangent to the zero force coefficient points. One such plate, for an AT-cut, is shown schematically in Figure 9. This figure shows a plate, initially round in outline, on to which four flats were ground on the perimeter. The flats are arranged to be paral-

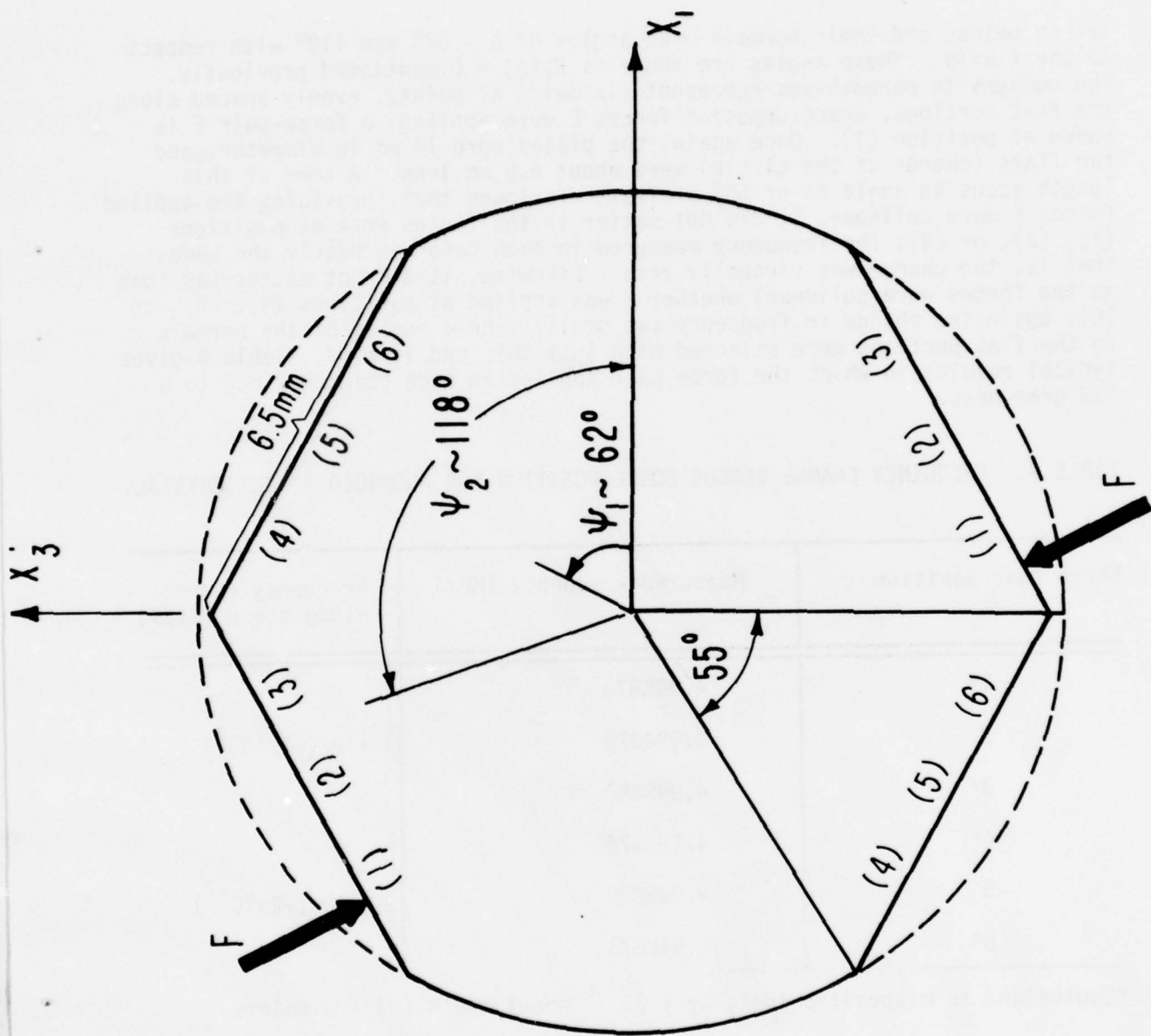


FIGURE 9. PROPOSED RHOMBOID CONFIGURATION FOR AT CUT.

1el in pairs, and their normals make angles of $\psi = 62^\circ$ and 118° with respect to the X axis. These angles are those of $K_f(\psi) = 0$ mentioned previously. The numbers in parentheses represent six pairs of points, evenly spaced along the flat portions, where opposing forces F were applied; a force-pair F is shown at position (1). Once again, the plates were 14 mm in diameter, and the flats (chords of the circle) were about 6.5 mm long. A cord of this length spans an angle $\Delta\psi$ of 55° . Tests disclosed that, providing the applied forces F were colinear, it did not matter if the forces were at positions (1), (2), or (3); the frequency measured in each case was nearly the same, that is, the change was virtually zero. Likewise, it did not matter (as long as the forces were colinear) whether F was applied at positions (4), (5), or (6); again the change in frequency was small. The ψ angles of the normals to the flat portions were selected with just this end in mind. Table 4 gives typical results in which the force pair applied at each point was due to a 130 gram mass.

TABLE 4. FREQUENCY CHANGE VERSUS FORCE POSITION FOR RHOMBOID AT CUT CRYSTAL.

Force pair position	Measured Frequency (MHz)	Frequency change along chord ($\Delta f/f$)
1*	4.998878	} $+1\text{Hz}(+2 \times 10^{-7})$
2	4.998879	
3*	4.998880	
4*	4.998874	} $-1\text{Hz}(-2 \times 10^{-7})$
5	4.998875	
6*	4.998875	

*Equivalent to mispositioning ψ by $\pm 27.5^\circ$ about the $K_f(\psi) = 0$ points.

Table 5 provides data obtained in a similar-type investigation, except, in this case, the experiment was repeated three times with a different force applied in each run and the measurements were taken at more closely spaced intervals.

As a result of these experiments we may conclude that if a distribution of forces along the flat edges of the crystal plate, acting along the normal to these edges, is applied to the crystal, the net frequency change will be minimal. This means that the flat edges can become the mounting surfaces, and that instead of a "two-point", or "four-point" mount, one can have instead "two-edge", or "four-edge" mounts. In addition, these mounts can span a considerable length, as shown for the above case in which the flat was 6.5 mm. The case of "four-edge" mounts follows directly from the "two-edge" case inasmuch as superposition of forces is known to hold, so it will not be expressly mentioned further.

TABLE 5. FREQUENCY CHANGE VERSUS FORCE MAGNITUDE FOR RHOMBOID AT CUT CRYSTAL.

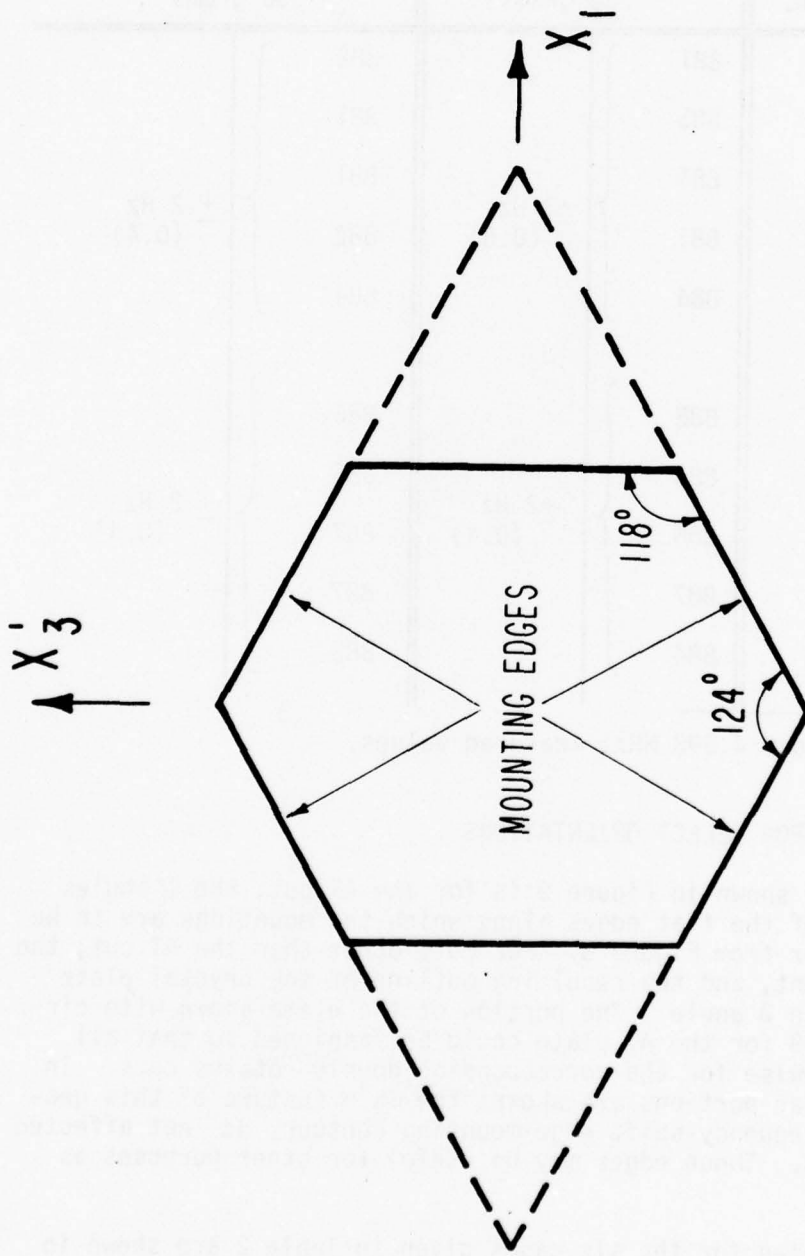
Force-pair position	Frequency* Hz	($\Delta f/f$) 10^{-6}	Frequency* Hz	($\Delta f/f$) 10^{-6}	Frequency* Hz	($\Delta f/f$) 10^{-6}
	130 grams		230 grams		330 grams	
1.0	884	+3 Hz (0.6)	881	+3 Hz (0.6)	882	+ 2 Hz (0.4)
1.5	883		883		881	
2.0	881		881		881	
2.5	881		881		882	
3.0	884		884		884	
4.0	884	-1 Hz (0.2)	888	+2 Hz (0.4)	886	+ 2 Hz (0.4)
4.5	885		884		885	
5.0	885		886		887	
5.5	885		887		887	
6.0	884		884		883	

* Frequency in hertz above 4.998 MHz; measured values.

SPECIFIC CONFIGURATIONS FOR SELECT ORIENTATIONS

The lateral contour shown in Figure 9 is for the AT cut; the ψ angles that fix the positions of the flat edges along which the mountings are to be made come from Table 2 or from Figure 5. For cuts other than the AT cut, the ψ values will be different, and the resulting outline of the crystal plate will likewise change with θ angle. The portion of the plate shown with circular outline in Figure 9 for the AT plate could be fashioned so that all edges are straight; likewise for the corresponding doubly rotated cuts. In the following, no circular portions are shown; the main feature of this geometry, i.e., the zero-frequency-shift edge mounting contour, is not affected by these unused portions. These edges may be useful for other purposes as will be described later.

The outlines generated for the six cases given in Table 2 are shown in Figures 10 to 15. The full outline determined by the ψ angles is the rhomboid shown for each case, including the dotted lines; the solid-lined figure



AT CUT ($\phi = 0^\circ$)

FIGURE 10. PLATE GEOMETRY FOR MINIMUM FORCE-FREQUENCY EFFECT; $\phi=0^\circ$. (AT CUT)

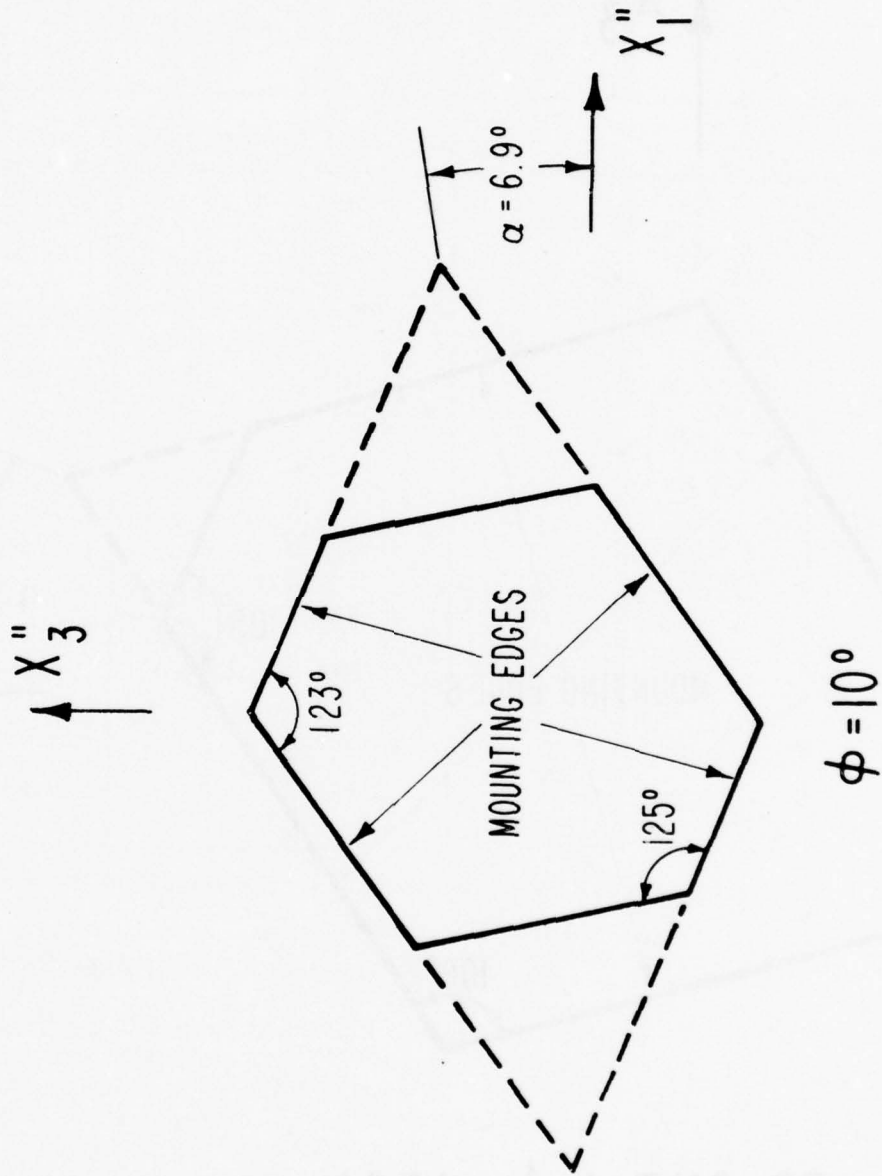
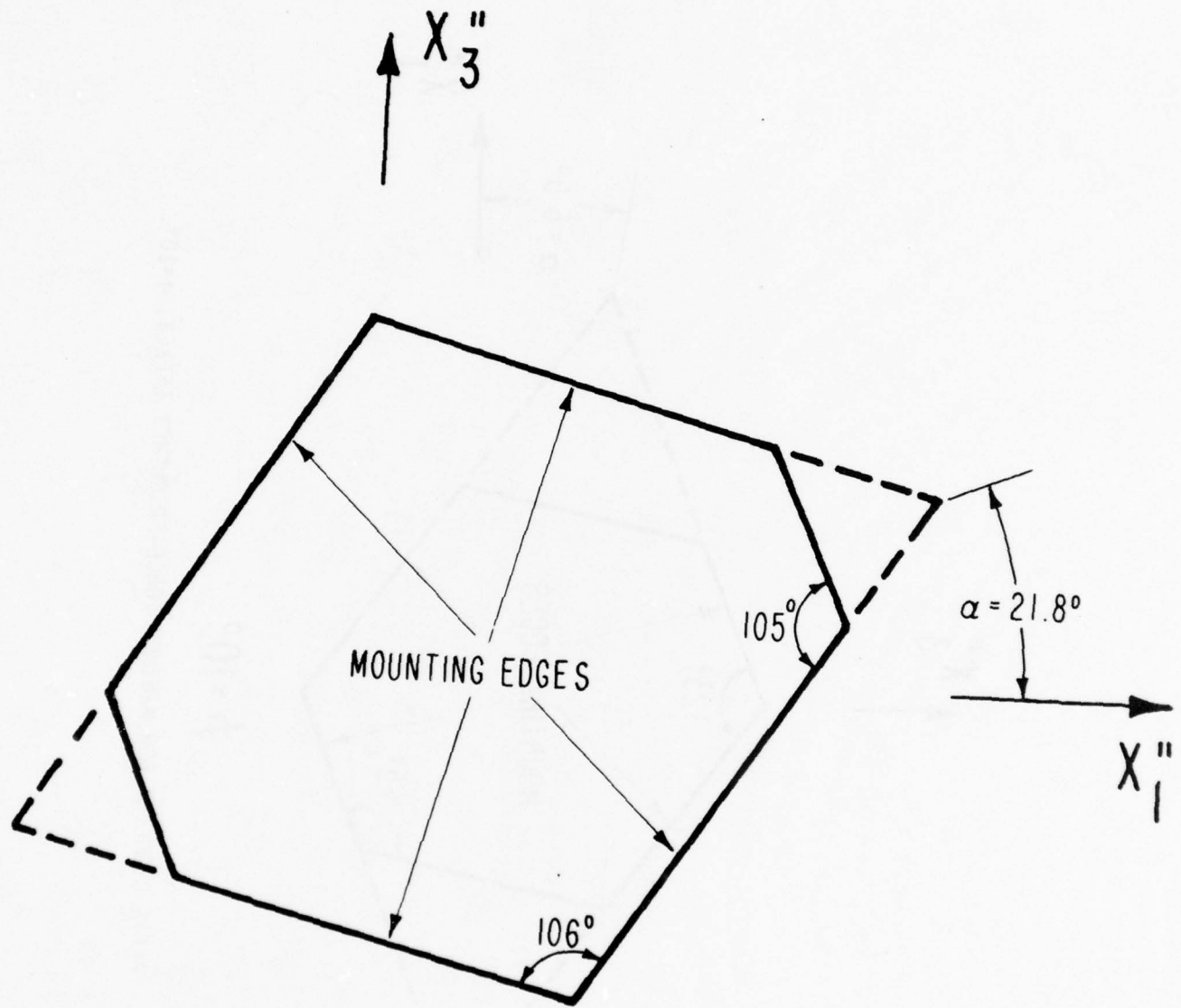
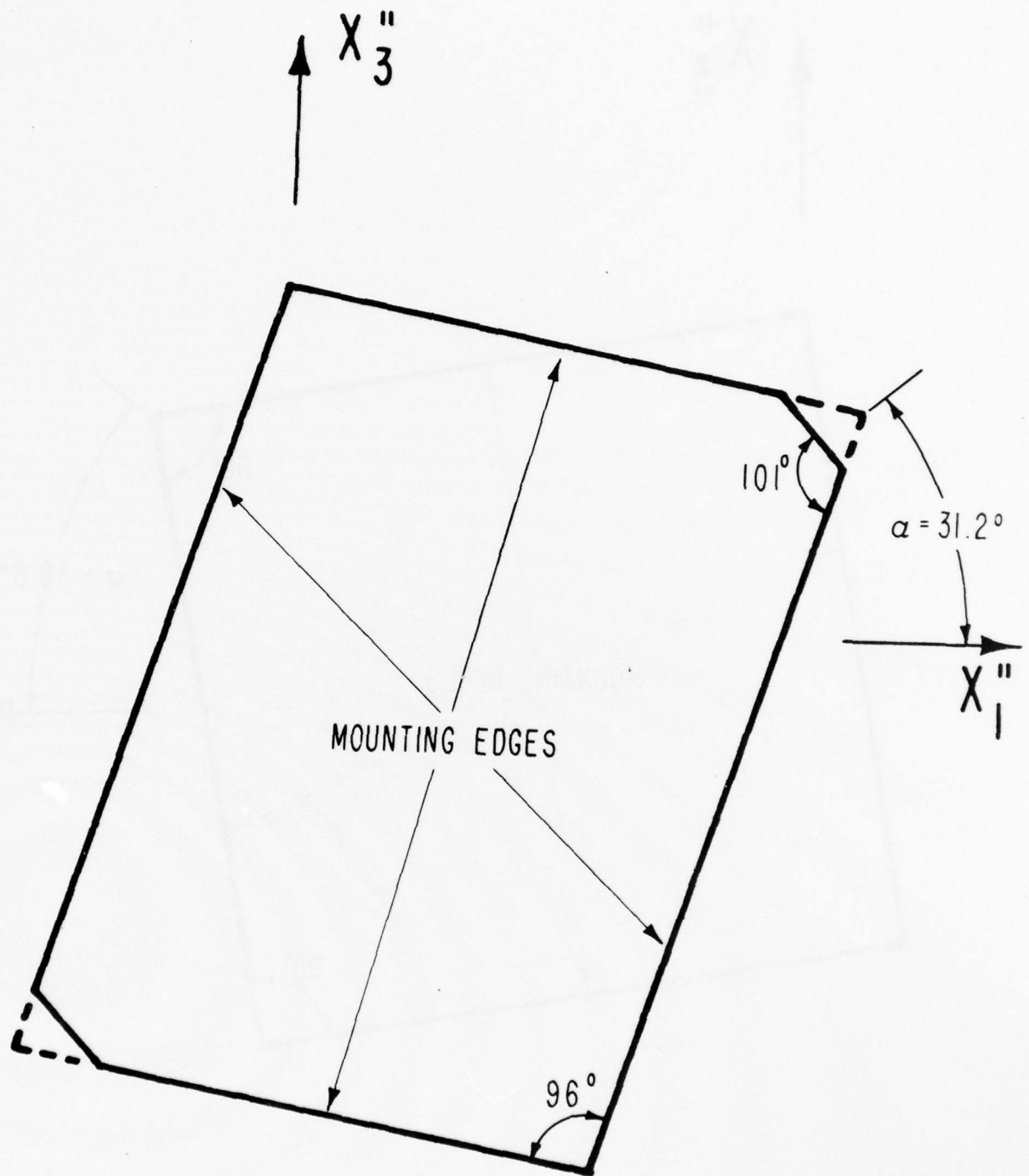


FIGURE 11. PLATE GEOMETRY FOR MINIMUM FORCE-FREQUENCY EFFECT; $\phi=10^\circ$.



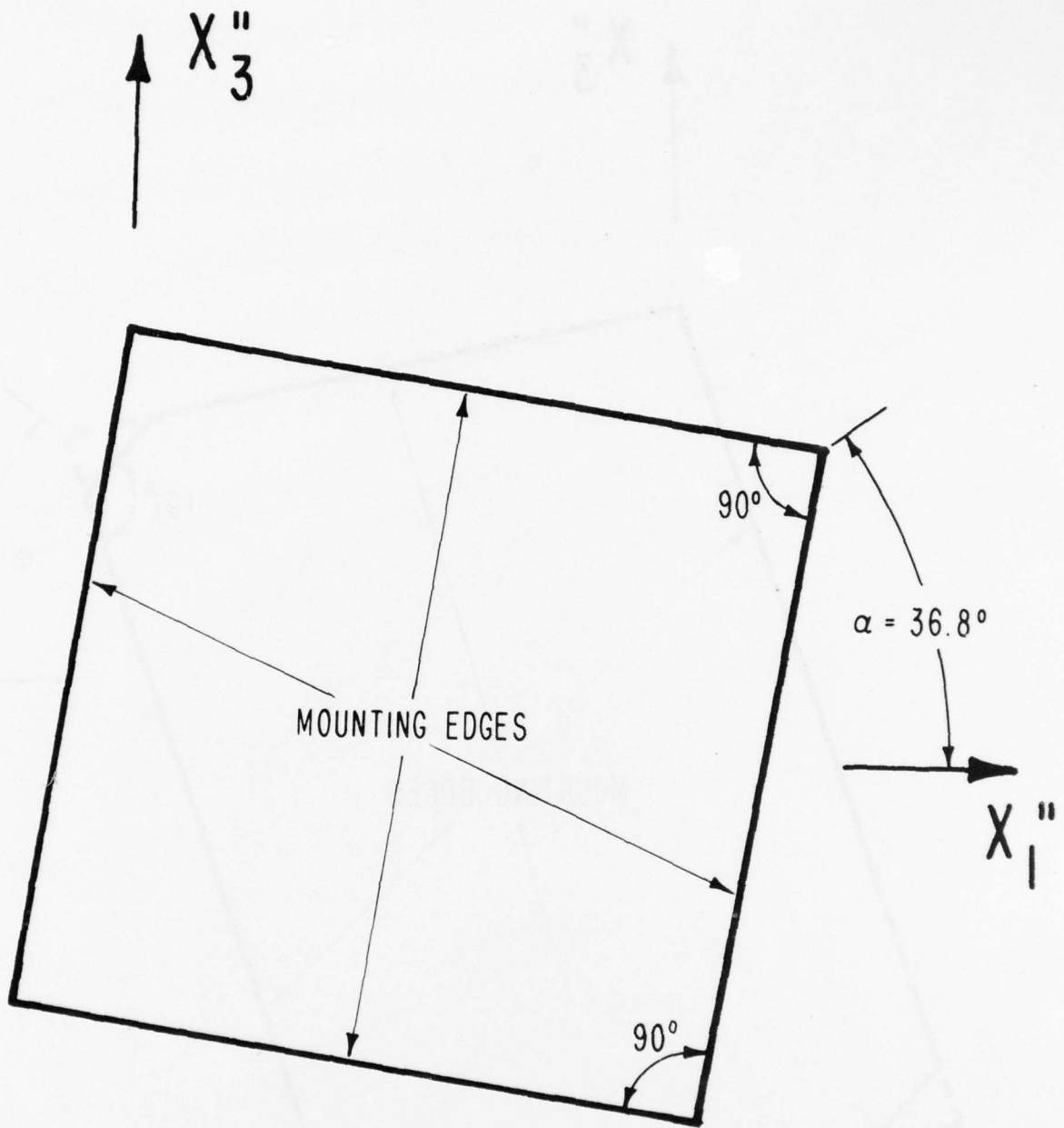
FC CUT ($\phi = 15^\circ$)

FIGURE 12. PLATE GEOMETRY FOR MINIMUM FORCE-FREQUENCY EFFECT; $\phi = 15^\circ$. (FC CUT)



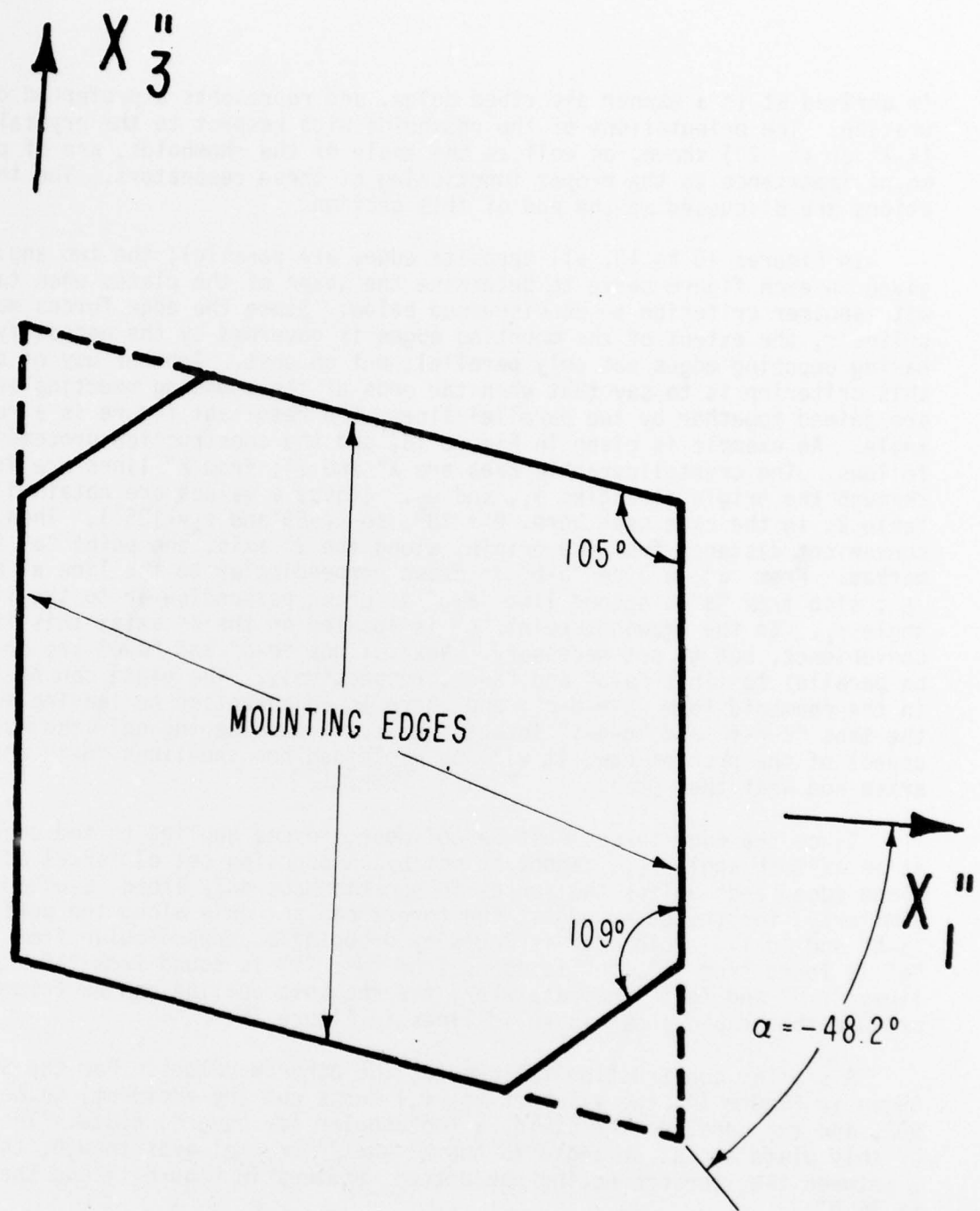
IT CUT ($\phi = 19.1^\circ$)

FIGURE 13. PLATE GEOMETRY FOR MINIMUM FORCE-FREQUENCY EFFECT; $\phi=19.1^\circ$. (IT CUT)



SC CUT ($\phi = 21.9^\circ$)

FIGURE 14. PLATE GEOMETRY FOR MINIMUM FORCE-FREQUENCY EFFECT; $\phi=21.9^\circ$. (SC CUT)



$$\phi = 30^\circ$$

FIGURE 15. PLATE GEOMETRY FOR MINIMUM FORCE-FREQUENCY EFFECT; $\phi = 30^\circ$.

is arrived at in a manner described below, and represents a preferred configuration. The orientations of the rhomboids with respect to the crystal axes (X, Z' or X'', Z'') shown, as well as the angle of the rhomboids, are of paramount importance to the proper functioning of these resonators. The inclinations are discussed at the end of this section.

In Figures 10 to 15, all opposite edges are parallel; the two angles given in each figure serve to determine the shape of the plates when taken with another criterion to be discussed below. Since the edge forces must be colinear, the extent of the mounting edges is governed by the necessity of having opposing edges not only parallel, but abreast. Another way of stating this criterion is to say that when the ends of the opposing mounting edges are joined together by two parallel lines, the resultant figure is a rectangle. An example is given in Figure 16, and the construction proceeds as follows. The crystallographic axes are X'' and Z'' ; from X'' lines are drawn through the origin at angles ψ_1 , and ψ_2 . (These ψ values are obtained from Table 2; in the case used here, $\theta = 10^\circ$, so $\psi_1 \approx 69^\circ$ and $\psi_2 \approx 125^\circ$). Then, at a convenient distance from the origin, along the Z'' axis, the point "a" is marked. From "a", a line "a-b" is drawn perpendicular to the line at angle ψ_1 ; also from "a" a second line "a-c" is drawn perpendicular to the line at angle ψ_2 . In the drawing, point "c" is located on the X'' axis; this is a convenience, but is not necessary. Next, lines "c-d" and "d-e" are drawn to be parallel to lines "a-b" and "a-c", respectively. The plate can be left in the rhomboid form "a-e-d-c", and there is an advantage to leaving some of the tabs "c-h-f" and "g-e-i" intact. However, considering only the mounting aspect of the problem now, it will be explained how the lines "g-i" and "f-h" arise and what they mean.

Since the edge forces must be colinear, forces applied to the edge "a-e" at an azimuth angle ψ_1 , cannot be met by an opposing set of forces acting along edge "c-d" unless the forces in question act only along "a-g" and "d-f". Similarly, for the other edges, the forces can act only along the portions "a-h" and "d-i". Point "f" is found by dropping a perpendicular from "a"; "g" is found from "d"; "h" is found from "d"; "i" is found from "a". Dotted lines "f-h" and "g-i" indicate where the rhomboid outline can be trimmed to produce the hexoid shown in solid lines in Figure 11.

A similar construction follows for the other θ values. For the SC cut, shown in Figure 14, the value of $(\psi_2 - \psi_1)$ turns out (by accident) to be nearly 90° , and the construction yields a rectangular (or square) plate. The edges of this plate are at an angle to the X'' and Z'' crystal axes though; the angle α between the line connecting the dotted vertices in Figure 14 and the X'' axis is 36.8° .

The angles can be found analytically as follows: With ψ_1 and ψ_2 the two given angles where $K_f(\psi)$ is zero, let $A = \cos(\psi_2 - \psi_1)$ and $B = (\sin \psi_2 / \sin \psi_1)$. Then find θ from $\cos \theta = \frac{1-A\sqrt{1-2A+B^2}}{1-A}$. The angle between the mounting edges is then $\pi - (\psi_2 - \psi_1)$; the angle between the mounting edge and the edge perpendicular to the ψ_1 line is $(\pi - \theta)$; the angle between the mounting edge and the edge perpendicular to the ψ_2 line is $\{\theta + (\psi_2 - \psi_1)\}$. In some cases the supplementary angle must be taken.

The angle between the line joining the dotted vertices in Figures 10 to 15, and the X'' axis specifies the inclination of the plate and is denoted α .

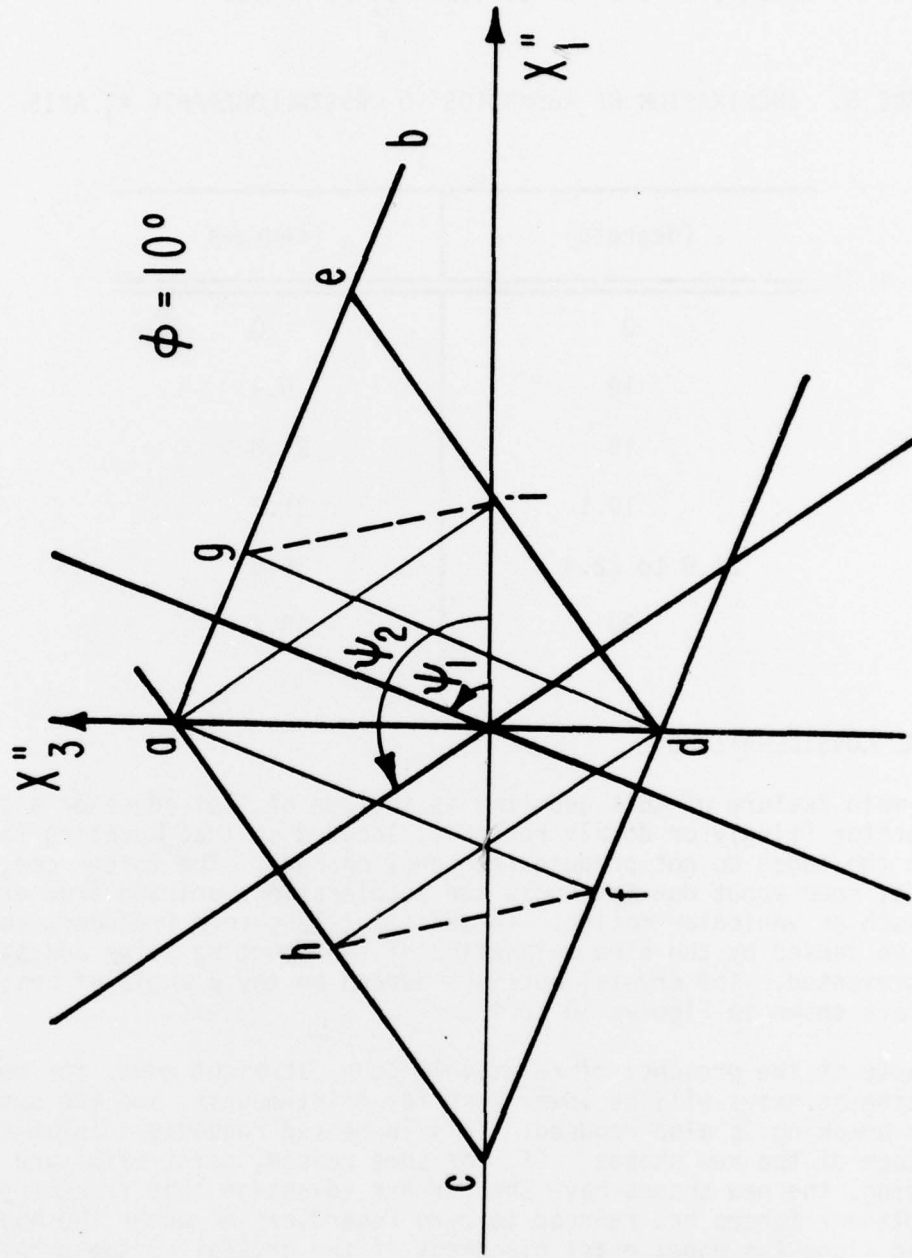


FIGURE 16. GENERALIZED CONSTRUCTION PROCEDURE APPLIED TO $\phi=10^\circ$ PLATE.

Values of this angle for the orientations shown in Figures 10 to 15 are given in Table 6. The angle α is equal to $(\psi_2 + \psi_1)/2 - \pi/2$.

TABLE 6. INCLINATION OF RHOMBOIDS TO CRYSTALLOGRAPHIC X_1^0 AXIS.

ϕ (degrees)	α (degrees)
0	0
10	6.9
15	21.8
19.1	31.2
21.9 to 22.4	36.8
30	- 48.2

ADDITIONAL CONSIDERATIONS

The main feature of this geometry is the use of flat edges on a crystal plate vibrator (singly or doubly rotated), located so that mounting forces acting at the edges do not produce frequency changes. The forces can, and usually do, come about due to shocks and accelerations arising from external sources such as vehicular motion. In addition, long-term frequency shifts, as might be caused by the slow relaxation of the mounting clips and supports, are also prevented. The crystal outlines depend on the ϕ angle of cut; some of these are shown in Figures 10 to 15.

Because of the presence of relatively long, straight edges for mounting, the mounting stresses will be lower than for point-mounts, and the susceptibility to breaking is also reduced. This increased ruggedness is an additional advantage of the new shapes. If, for some reason, point clips are used for mounting, the new shapes have the further advantage that frequency changes due to colinear forces are reduced to zero regardless of where the mounts are positioned along the edge; exact placement of the crystal at the proper place in the mount is not required (cf. Table 5). If, as will usually be the case, the crystal is mounted by clips extending over a portion of the mounting edges, then placement of the crystal in the mount is very easily and rapidly accomplished, since it is unnecessary to orient the crystal with respect to the mounting clips as in present designs. This is because the edges have been designed with the proper orientation already.

In the above description the plates were provided with four flat portions, while the remaining portions of the periphery were left circular (as in Figure 9), were trimmed off to make hexoid shapes (as in Figures 10 to 15),

or were left as rhomboid shapes (dotted lines in Figures 10 to 15). There are at least two reasons for modifying the non-mounting edges further; (1) mode spectrum control, and (2) placement of electrode tabs.

(1) Mode spectrum control - A plot of the crystal resonator admittance versus frequency is called the mode spectrum. For oscillator, and more particularly, filter applications, it is desirable that the resonator have a spectrum that contains as few extra resonances as possible. The mode spectra of acceptable and non-acceptable crystals in this regard are shown in Figure 17. Production of good filter crystals depends upon a number of factors, derived from theoretical considerations that collectively go under the name "energy trapping". Several important factors that contribute to energy trapping are:

- plate size and shape, and edge bevel
- electrode size and shape
- electrode thickness
- position of the electrode tabs.

Without going into details at this time, it may be very advantageous to have the clipped-off portions of the rhomboid extend beyond the dotted lines in Figure 16. These dotted lines were determined by considerations of colinear edges forces, and it was pointed out that the edges "h-c", "c-f", "i-c", and "e-g" were of no use in this regard. For the purposes of energy trapping, it may be advisable to clip off the non-mounting edges so that they are parallel to "f-h" and "i-g", but at locations closer to points "c" and "e", respectively. This is shown in Figure 18 for the case of the AT cut, although the feature is generic to all the cuts from $\theta=0^\circ$ to $\theta=30^\circ$. Instead of cutting along "f-h" and "i-g", the cuts would be made along the primed, or double-primed lines. Mounting clips would only extend over those portions of the mounting edges where the force-arrows are shown in Figure 18.

(2) Placement of electrode tabs - Electrodes are usually deposited on the crystal surface in a "keyhole" pattern, with overlapping central portions and "tabs" that do not overlap; (see Figure 19). The azimuth angle of the electrode tabs is important in at least two ways: (1) mode spectrum control and (2) temperature gradient compensation. The azimuth angle is the acute angle between the tabs and the crystal X_1 axis. This angle plays a role in controlling the spectrum of a resonator, although for doubly rotated crystals this is not very well understood yet.

Temperature gradients in the thickness direction of a vibrator produce frequency changes as large as those produced by external forces and accelerations²³. For the doubly rotated cut at $\theta=21.9^\circ$ to 22.4° this effect vanishes, and permits thermal-transient-compensated crystals for fast warmup oscillators and advanced frequency standards. For these crystals, however, thermal gradients in the lateral direction are not compensated, and do produce frequency shifts. Orienting the electrode tabs in azimuth may minimize this. The tabs would then extend into the lengthened portion of the hexoid crystals as seen in Figure 20, where they may conveniently be connected to the external circuit. If the tabs can be brought out to the mounting portions of the

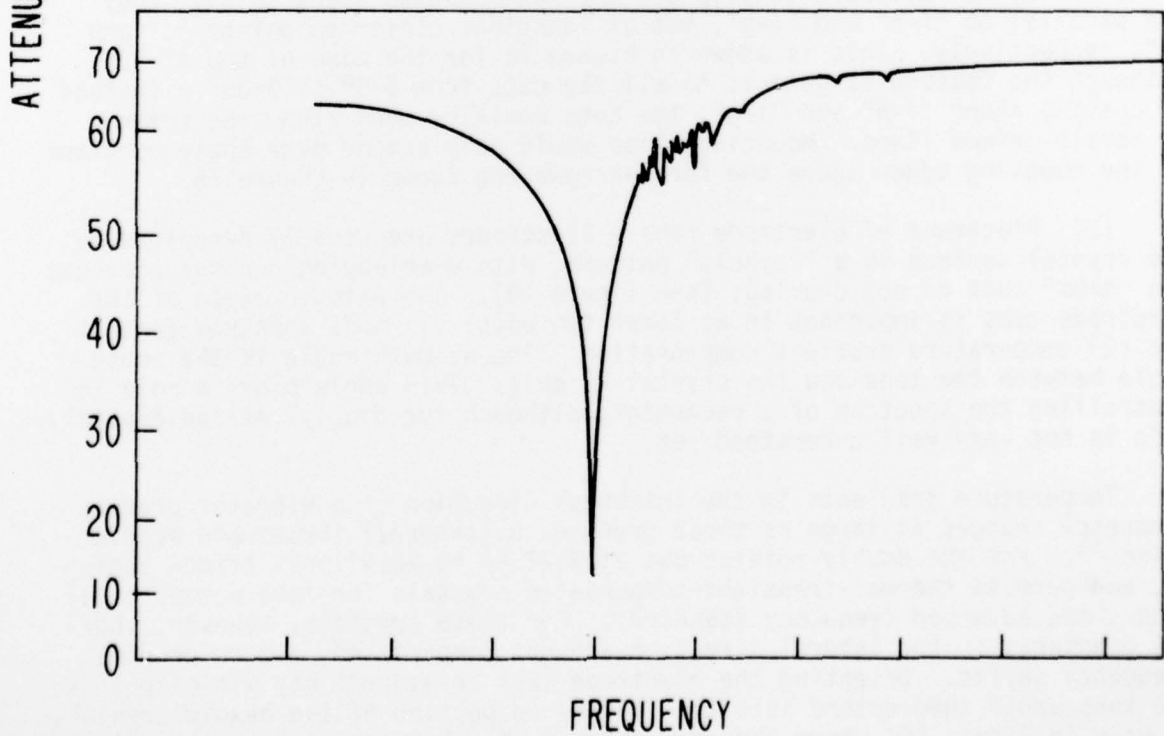
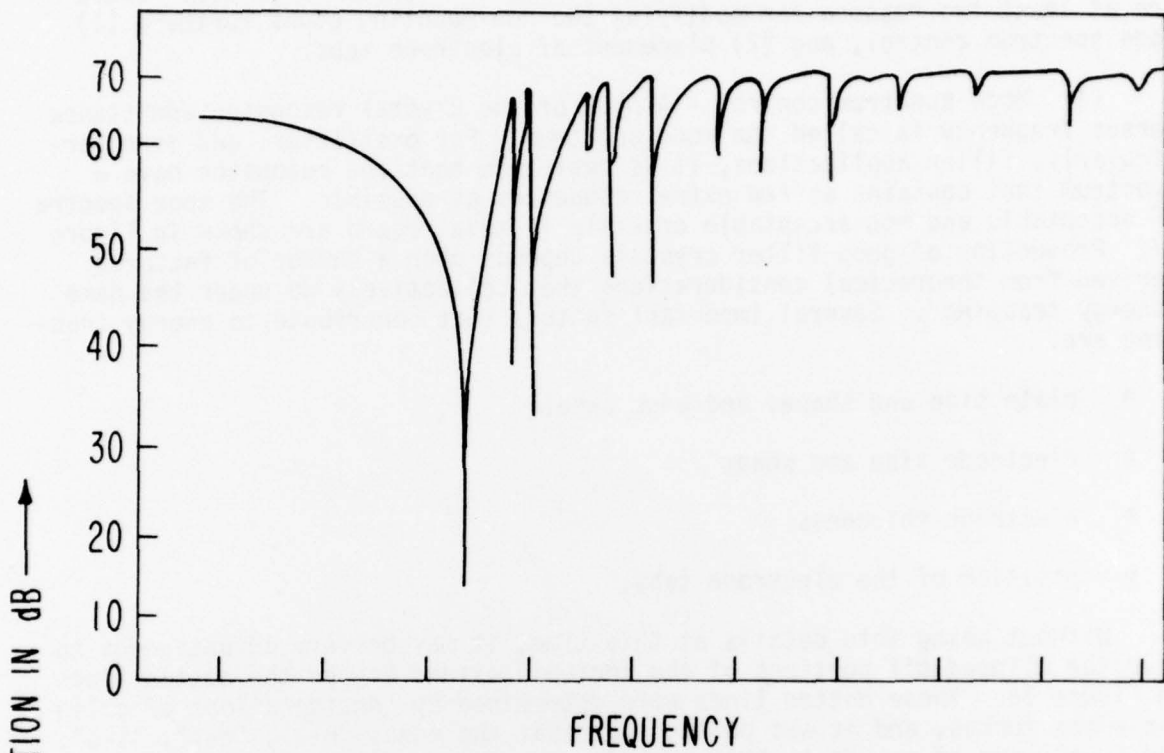
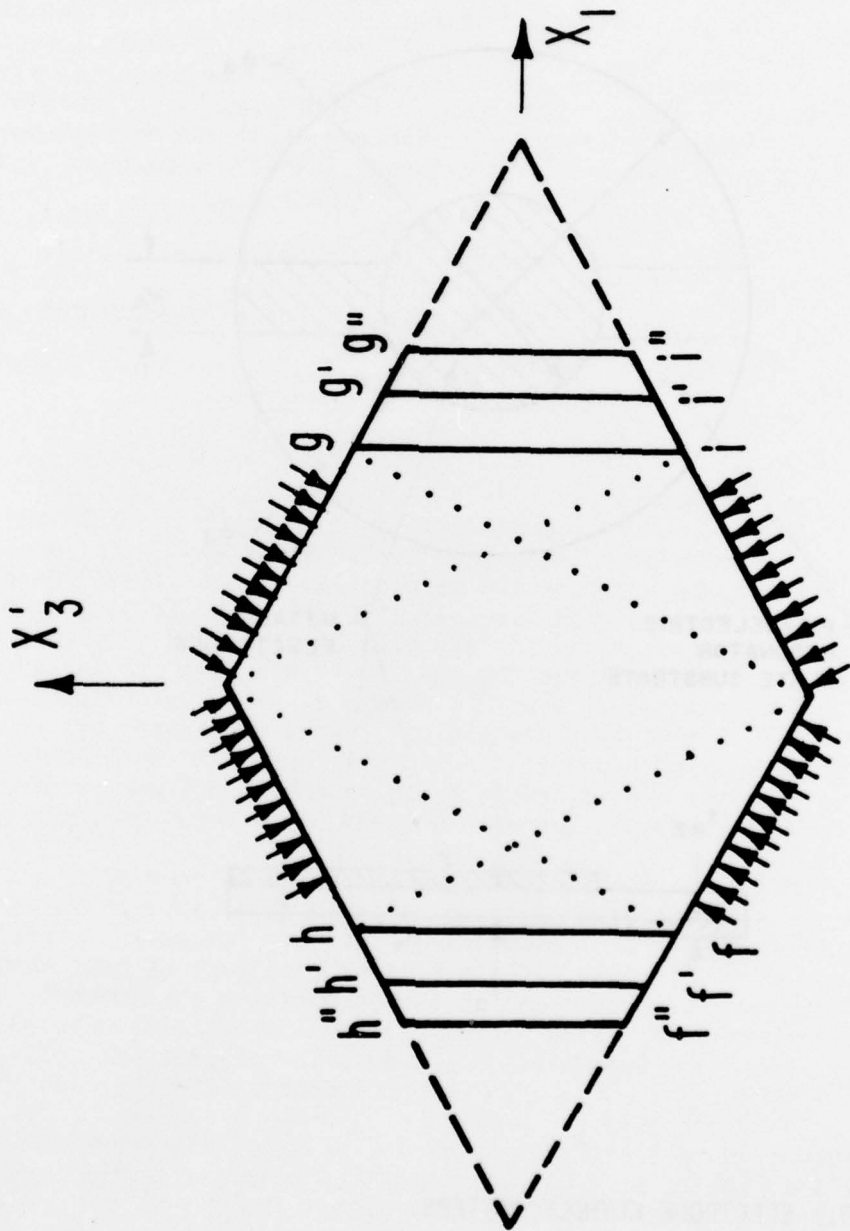


FIGURE 17. MODE SPECTROGRAPH COMPARISON.



AT CUT ($\phi = 0^\circ$)

FIGURE 18. MODIFICATION OF GEOMETRY FOR ENERGY TRAPPING PURPOSES.

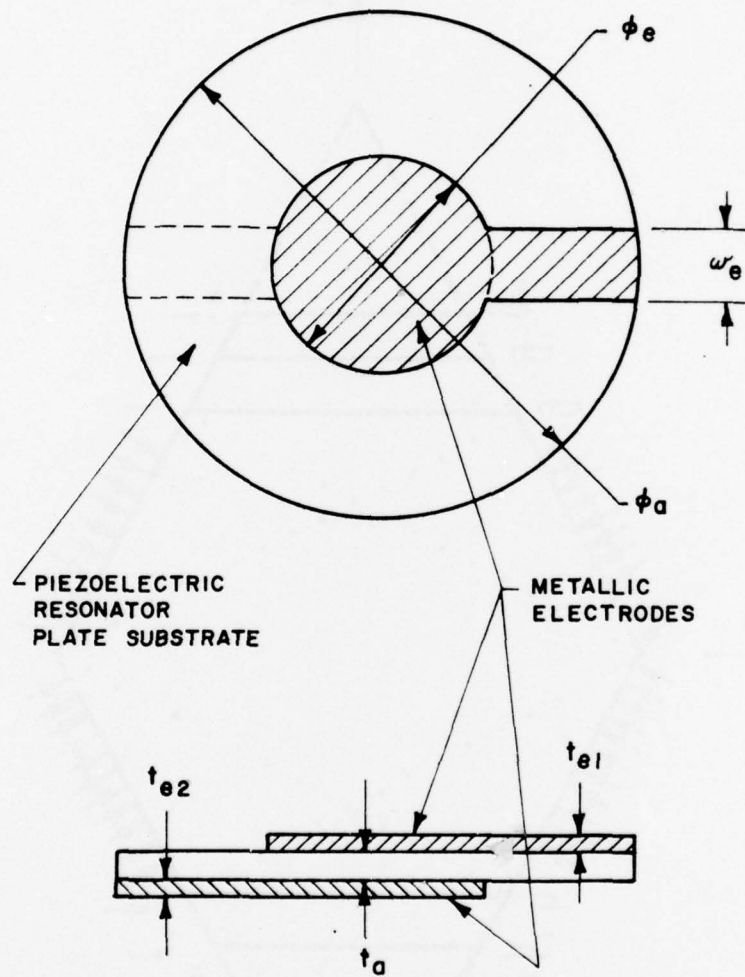


FIGURE 19. ELECTRODE KEYHOLE PATTERN.

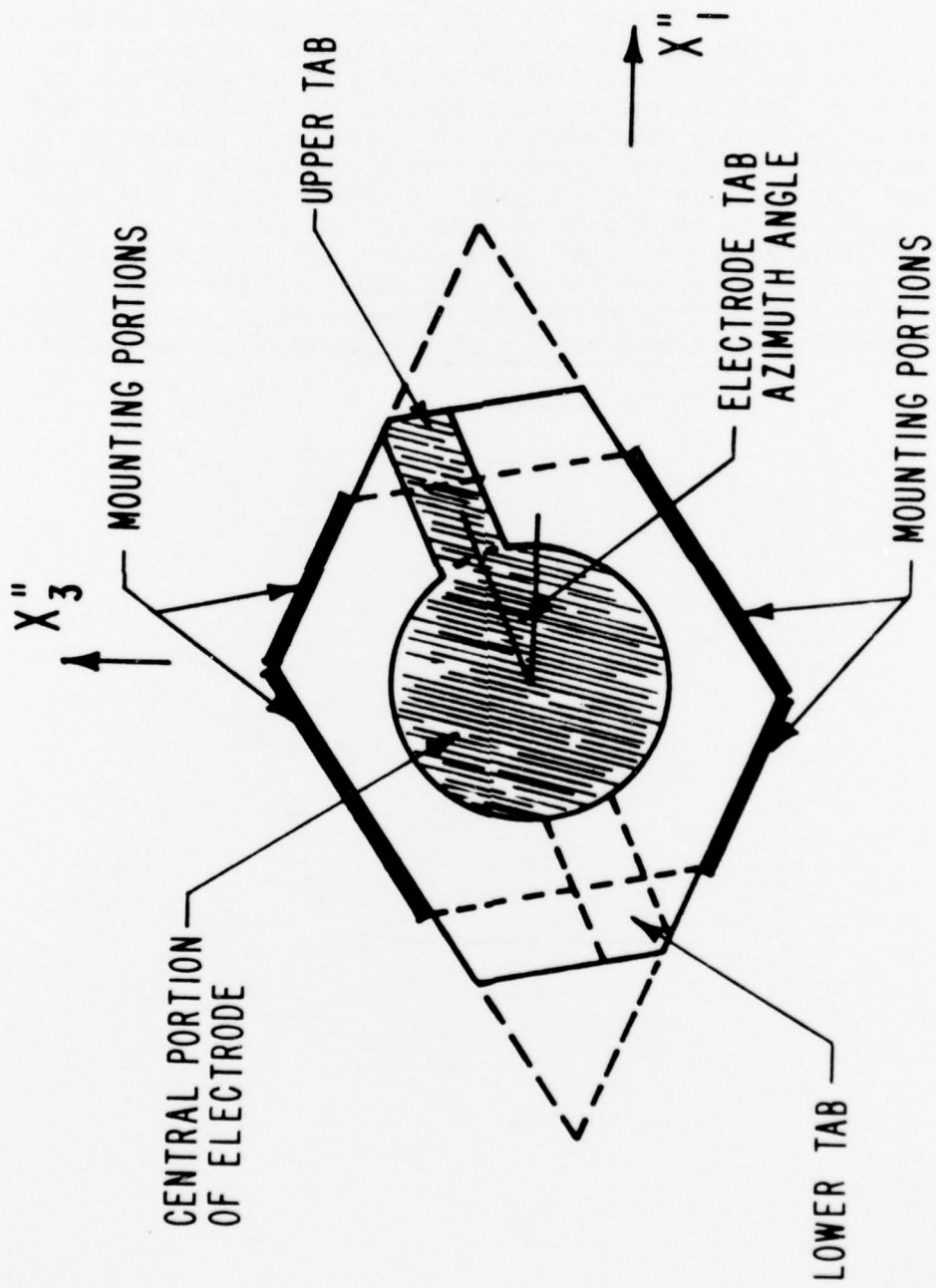


FIGURE 20. HEXOID RESONATOR WITH OFF-AXIS ELECTRODE TABS.

mounting edges, then the mounts can be used for the electrical connections, as is usual for resonators.

CONCLUSIONS

This report describes in detail a design for resonator plates having a prescribed lateral contour, with mounting surfaces provided along relatively large portions of the periphery, so that mounting stresses are greatly reduced in size with no detriment to the force immunity of the older type of mounting. A different lateral contour, of rhomboid configuration, for each and every member of the doubly rotated family of quartz cuts located on the zero temperature coefficient locus extending from the AT-cut to the rotated-X-cut is provided. It is shown that a crystal of 14mm diameter, with this configuration, can be bonded along a 6.5 mm edge (effective $\Delta\psi$ of 55°), which, when subjected to an increased force of 300 per cent, still exhibits less frequency change than the older type mounts even when $\Delta\psi$ is kept less than $\pm 5^\circ$. Finally, the effects of truncating the plates edges on the mode spectrum, and for thermal gradient compensation of the quartz plate, are considered.

REFERENCES*

1. V.E. Bottom, "Note on the Anomalous Thermal Effect in Quartz Oscillator Plates", American Mineralogist, Vol. 32, Nos. 9 and 10, September-October 1947, pp. 590-591.
2. E.A. Gerber, "Precision Frequency Control for Guided Missiles", Proc. 1st IRE National Convention on Military Electronics, Session 6, June 1957, pp. 91-98.
3. E.A. Gerber, "Reduction of Frequency-Temperature Shift of Piezoelectric Crystals by Application of Temperature-Dependent Pressure", Proc. IRE, Vol. 48, No. 2, February 1960, pp. 244-245.
4. A.D. Ballato and R. Bechmann, "Effect of Initial Stress in Vibrating Quartz Plates", Proc. IRE, Vol. 48, No. 2, February 1960, pp. 261-262.
5. A.D. Ballato, "Effects of Initial Stress on Quartz Plates Vibrating in Thickness Modes", Proc. 14th AFCS, May-June 1960, pp. 89-114.
6. E.A. Gerber and M.H. Miles, "Temperature Compensation of Piezoelectric Resonators by Mechanical Stress", Proc. 15th AFCS, May-Jun 1961, pp. 49-65.
7. E.A. Gerber and M.H. Miles, "Reduction of the Frequency-Temperature Shift of Piezoelectric Resonators by Mechanical Stress", Proc. IRE, Vol. 49, No. 11, November 1961, pp. 1650-1654.
8. C.R. Mingins, R.W. Perry, and L.C. Barcus, "Effects of External Forces (Transient and Permanent)", Quarterly Report No. 1 on Contract No. DA28-043-AMC-01240(E), 1 May to 31 July 1965, US Army Electronics Command, Fort Monmouth, NJ 07703.
9. C.R. Mingins, R.W. Perry, and L.C. Barcus, "Effects of External Forces (Transient and Permanent)", Quarterly Report No. 2 on Contract No. DA28-043-AMC-01240(E), 1 August to 31 October 1965, US Army Electronics Command, Fort Monmouth, NJ 07703.
10. C.R. Mingins, R.W. Perry, and L.C. Barcus, "Effects of External Forces (Transient and Permanent)", Quarterly Report No. 3 on Contract No. DA28-043-AMC-01240(E), 1 November 1965 to 31 January 1966, US Army Electronics Command, Fort Monmouth, NJ 07703.
11. C.R. Mingins, R.W. Perry, and L.C. Barcus, "Effects of External Forces (Transient and Permanent)" Final Report on Contract DA28-043-AMC-01240(E), 3 May 1965 to 2 May 1966, US Army Electronics Command, Fort Monmouth, NJ 07703; "Transient Reactions to Stress Changes in Vibrating Crystal Plates", Proc. 20th AFCS, April 1966, pp. 50-69.
12. J.M. Ratajski, "The Force Sensitivity of AT-Cut Quartz Crystals", Proc. 20th AFCS, April 1966, pp. 33-49.

*AFCS: Annual Frequency Control Symposium, US Army Electronics R&D Command, Fort Monmouth, NJ 07703

13. R.W. Keyes and F.W. Blair, "Stress Dependence of the Frequency of Quartz Plates", Proc. IEEE, Vol. 55, No. 4, April 1967, pp. 565-566.
14. J.M. Ratajski, "Force-Frequency Coefficient of Singly-Rotated Vibrating Quartz Crystals, " IBM J. Res. Dev., Vol. 12, No. 1, January 1968, pp. 92-99.
15. P.C.Y. Lee, Y.S. Wang, and X. Markenscoff, "Elastic Waves and Vibrations in Deformed Crystal Plates", Proc. 27th AFCS, June 1973, pp. 1-6.
16. P.C.Y. Lee, Y.S. Wang, and X. Markenscoff, "Effects of Initial Bending on the Resonance Frequencies of Crystal Plates", Proc. 28th AFCS, May 1974, pp. 14-18.
17. P.C.Y. Lee and D.W. Haines, "Piezoelectric Crystals and Electroelasticity", in R.D. Mindlin and Applied Mechanics, (G. Herrmann, ed.) Pergamon Press, New York, 1974, pp. 227-253.
18. P.C.Y. Lee, Y.S. Wang, and X. Markenscoff, "High Frequency Vibrations of Crystal Plates under Initial Stresses", J. Acoust. Soc. Amer., Vol. 57, No. 1, Jan 1975, pp. 95-105.
19. P.C.Y. Lee, Y.S. Wang, and X. Markenscoff, "Nonlinear Effects of Initial Bending on the Vibrations of Crystal Plates", J. Acoust. Soc. Am., Vol. 59, No. 1, Jan 1976, pp. 90-96.
20. P.C.Y. Lee, "Some Problems in Vibrations of Piezoelectric Crystal Plates", Report on the Workshop on Application of Elastic Waves in Electrical Devices, Non-Destructive Testing and Seismology, (J.D. Achenbach, Y.H. Pao, and H.F. Tiersten, eds.), Northwestern University, Evanston, Illinois 60201, May 1976, pp. 442-489.
21. A. Ballato, E.P. EerNisse, and T. Lukaszek, "The Force-Frequency Effect in Doubly Rotated Quartz Resonators", Proc. 31st AFCS, June 1977, pp.8-16.
22. A. Ballato, T. Lukaszek, and E.P. EerNisse, "Force-Frequency and Other Effects in Doubly Rotated Vibrators", Technical Report ECOM-4536, US Army Electronics Command, Fort Monmouth, NJ 07703, September 1977, 45 pp.
23. A. Ballato, "Doubly Rotated Thickness Mode Plate Vibrators", in Physical Acoustics: Principles and Methods, (W.P. Mason and R.N. Thurston, eds.), Vol. 13, Chap. 5. Academic Press, New York, 1977, pp. 115-181.
24. E.P. EerNisse, T. Lukaszek, and A. Ballato, "Variational Calculation of Force-Frequency Constants of Doubly Rotated Quartz Resonators", IEEE Trans. Sonics Ultrason., Vol. SU-25, No.3, May 1978, pp. 132-138.
25. D. Janiaud, L. Nissim, and J.-J. Gagnepain, "Analytical Calculation of Initial Stress Effects on Anisotropic Crystals: Application to Quartz Resonators", Proc. 32nd AFCS, May-June 1978, pp. 169-179.
26. E.P. EerNisse, "Rotated X-Cut Quartz Resonators for High Temperature Applications," Proc. 32nd AFCS, May-June 1978, pp. 255-259.

27. A. Ballato, "Force-Frequency Compensation Applied to Four-Point Mounting of AT-Cut Resonators", IEEE Trans. Sonics Ultrason., Vol. SU-25, No. 4, July 1978, pp. 223-226.